

Topological Defects in Anisotropic Driven Open Systems

L. M. Sieberer^{1,2,3,*} and E. Altman¹

¹*Department of Physics, University of California, Berkeley, California 94720, USA*

²*Institute for Theoretical Physics, University of Innsbruck, A-6020 Innsbruck, Austria*

³*Institute for Quantum Optics and Quantum Information of the Austrian Academy of Sciences, A-6020 Innsbruck, Austria*

We study the dynamics and unbinding transition of vortices in the compact anisotropic Kardar-Parisi-Zhang (KPZ) equation. The combination of non-equilibrium conditions and strong spatial anisotropy drastically affects the structure of vortices and amplifies their mutual binding forces, thus stabilizing the ordered phase. We find novel universal critical behavior in the vortex-unbinding crossover in finite-size systems. These results are relevant for a wide variety of physical systems, ranging from strongly coupled light-matter quantum systems to dissipative time crystals.

Introduction.—The celebrated theory of Kosterlitz and Thouless (KT) highlights the crucial role that is played by topological defects in the phase transition of U(1)-symmetric and short-range interacting two-dimensional (2D) systems in thermal equilibrium. At low temperatures, topological defects (vortices) of opposite charge form tightly bound pairs, while they are free to roam and destroy order at high temperatures. For the stability of the ordered phase, it is crucial that vortices interact like charged particles, i.e., with a Coulomb force that decays as $\sim 1/r$. In particular, any faster decay at large distances would destabilize the ordered phase.

Interestingly, such a qualitative change of the vortex interaction can be induced by taking the system out of thermal equilibrium. This has been studied extensively in the context of the complex Ginzburg-Landau equation (CGLE) [1] and the compact KPZ (cKPZ) equation [2, 3] (the former can be reduced to the latter in the long-wavelength limit [4, 5]). The extent to which these equations violate equilibrium conditions can be quantified in terms of a single parameter that determines the strength of the characteristic non-linearity in the cKPZ equation [6–10]. Due to this non-linear term, the vortex interaction is exponentially screened at large distances — thus, the ordered phase ceases to exist. This finding is particularly relevant, since the cKPZ equation is the long-wavelength description of a vast variety of systems, ranging from “polar active smectics” or “moving stripes” [11], to driven-dissipative condensates such as exciton-polaritons [3, 8–10, 12–19], synchronization in arrays of limit-cycle oscillators [20], and limit-cycle phases that emerge from a Hopf bifurcation [21–25] — such phases have attracted a lot of attention recently and could be coined dissipative time crystals [26].

In this paper, we report that breaking *rotational* symmetry has an equally strong impact on the form of the vortex interaction, and acts to *stabilize* the ordered phase. This is highly significant for the systems mentioned above, in which spatial anisotropy is either intrinsic or can be imposed deliberately. The change in the vortex interaction can be understood intuitively by

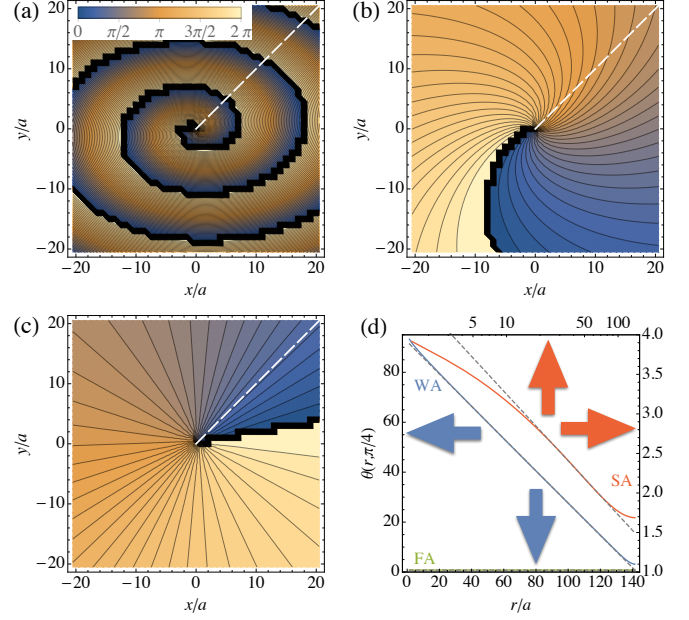


Figure 1. (Color online) Single vortices in the cKPZ equation. (a) Weakly anisotropic (WA) regime with $\alpha_x = \lambda_x/(2D) \approx 0.9$ and $\alpha_y = \lambda_y/(2D) \approx 0.4$ in Eq. (2). The vortex has a squeezed spiral structure with a clearly visible radially emitted wave. (b) Strongly anisotropic (SA), $\alpha_x \approx 0.9$, $\alpha_y \approx -0.4$. The spiral structure is pronounced only at short distances from the vortex core. (c) In the fully anisotropic (FA) case, with $\alpha_x = -\alpha_y \approx 0.7$, there is no radial wave. We note, that (a-c) are equally non-linear in the sense that $\alpha_x^2 + \alpha_y^2 = 1$. (d) Radial dependence of the vortex field $\theta(r, \phi)$ along the dashed line in (a-c). $\theta(r, \pi/4)$ grows linearly in the WA regime (a), logarithmically in the SA regime (b) (note the logarithmic r -axis), and is constant at the FA point. The dashed lines are linear fits which agree well with the data up to finite-size effects at large distances.

considering the mere structure of a single topological defect shown in Fig. 1. In the *isotropic* cKPZ equation, defects are “radiative,” i.e., they emit waves radially away from the core, giving them a spiral structure (Fig. 1(a)). Perturbations, e.g., due to the presence of another defect, decay exponentially in the upstream direction of traveling waves — heuristically, this explains why the interaction between vortices is exponen-

* lukas.sieberer@gmail.com

tially screened [2]. As we show below, the radially emitted wave decays away from the vortex core for sufficiently strong anisotropy (Fig. 1(b)), and is completely absent in a *fully anisotropic* configuration (Fig. 1(c)). Then, vortices in the *anisotropic* cKPZ (caKPZ) are similar to the ones in equilibrium systems (up to an anisotropic deformation). We expect their interactions to be long-range and, therefore, order to be stable, as also indicated by numerical simulations [4, 5].

However, in a non-linear theory such as the caKPZ equation, single-vortex solutions cannot simply be superposed to yield multi-vortex solutions, and in the latter additional features may appear that cannot be anticipated from the former. Below, we present an analytical calculation of the interaction between defects, based on a recently developed mapping to a dual electrodynamics problem [3, 15]. This perturbative calculation is valid up to an exponentially large characteristic scale, and it shows that the attraction between oppositely charged vortices is even enhanced as compared to the linear (i.e., thermal equilibrium) isotropic case. For this enhancement to occur, the combination of non-linearity and anisotropy is essential. In fact, as explained above, the non-linearity alone would give a repulsive correction to the interaction, while anisotropy in a linear theory can simply be absorbed in an anisotropic rescaling of the units of length and does not have any relevant qualitative effect on the form of the interaction.

Based on the modified vortex interaction, we derive renormalization group (RG) equations that describe the vortex-unbinding crossover in systems that are fully anisotropic and smaller than the characteristic scale. Since this scale is parametrically large, we expect that the universal critical behavior we find will be observed in experiments and numerical investigations of the caKPZ equation. In particular, the divergence of the correlation length is in between the essential singularity characteristic of the KT transition and true scaling behavior as in usual continuous phase transitions.

Previous studies of the caKPZ equation [8, 9, 11, 18] assumed that vortices do not proliferate on the characteristic scale of the RG flow of the non-compact equation [11, 27], and can hence be included *a posteriori* in an emergent equilibrium description. This assumption, however, breaks down close to the unbinding transition, where vortices are the dominant fluctuations. To access this region, we focus on the combined impact of non-linearity and strong anisotropy on the vortex dynamics.

Model.—The caKPZ equation reads

$$\partial_t \theta = \sum_{i=x,y} \left[D_i \partial_i^2 \theta + \frac{\lambda_i}{2} (\partial_i \theta)^2 \right] + \eta, \quad (1)$$

where η is Gaussian noise with zero mean and correlations $\langle \eta(\mathbf{r}, t) \eta(\mathbf{r}', t') \rangle = 2\Delta \delta(\mathbf{r} - \mathbf{r}') \delta(t - t')$. θ is a compact variable, i.e., one that admits topological defects. In physical realizations, θ may be the phase field in driven-open condensates [3, 8–10, 12–18], in limit-cycle phases [21–25] or in oscillator arrays. In the latter

case, Eq. (1) emerges as the continuum limit of the noisy Kuramoto-Sakaguchi model [20, 28, 29] with anisotropic couplings between the oscillators. θ may also represent the displacement field in polar active smectics [11].

For stability, we require $D_{x,y} > 0$, while $\lambda_{x,y}$ are unrestricted; in the following, we set $D_x = D_y = D$, which can always be achieved by an anisotropic rescaling of the units of length. For $\lambda_x = \lambda_y = 0$, Eq. (1) reduces to the (continuum limit of the) XY model with dissipative dynamics [30]. We denote $\lambda_{x,y}$ having the same and opposite signs as *weakly anisotropic* (WA) and *strongly anisotropic* (SA) regimes, respectively. In particular, we denote the configuration with $\lambda_x = -\lambda_y$ as *fully anisotropic* (FA). We shall restrict ourselves to small values of $|\lambda_{x,y}|$ in order to avoid a dynamical instability of Eq. (1) [16, 20]. In systems described by Eq. (1) with $\lambda_x = \lambda_y$, the ordered phase is always destroyed in the thermodynamic limit by the proliferation of vortices [2, 3, 31]. Here, we investigate whether order can be stable if $\lambda_x \neq \lambda_y$.

Structure of a single vortex.—A vortex is a solution of Eq. (1) without noise that is stationary up to uniform oscillations with a frequency ω_0 ,

$$\partial_t \theta = D \nabla^2 \theta + \frac{\lambda_x}{2} (\partial_x \theta)^2 + \frac{\lambda_y}{2} (\partial_y \theta)^2 - \omega_0 = 0, \quad (2)$$

and obeys $\oint d\mathbf{l} \cdot \nabla \theta = 2\pi$ for any integration path that surrounds the vortex core. We solve Eq. (2) numerically by discretizing it on a lattice (see [32] for details). In addition, we determine analytically the asymptotic behavior of $\theta(r, \phi)$ for $r \rightarrow \infty$ at fixed polar angle ϕ , which takes the form

$$\theta(r, \phi) = k_0(\phi)r + b(\phi) \ln(r/a) + \Phi(\phi) + O(1/r), \quad (3)$$

where $k_0(\phi)$ is the (anisotropic) asymptotic wave number, $b(\phi)$ the coefficient of the first sub-leading correction, and $\Phi(\phi)$ contains the topological part of the vortex field. a is a microscopic cutoff scale such as the lattice spacing in oscillator arrays, or the healing length in driven-open condensates. As illustrated in Fig. 1(a,d), in the WA regime, we find a squeezed spiral structure with [32]

$$k_0(\phi) = -\sqrt{\frac{2\omega_0}{\lambda_x \cos(\phi)^2 + \lambda_y \sin(\phi)^2}}, \quad (4)$$

where ω_0 is determined by the regularization at short distances [2]. In the SA regime shown in Fig. 1(b,d), when one of $\lambda_{x,y}$ is negative, Eq. (4) implies $k_0(\phi) = \omega_0 = 0$. The leading asymptotic behavior is then given by the logarithmic term in Eq. (3) with $b(\phi) = b_0 = \text{const}$. Finally, for FA parameters $\lambda_x = -\lambda_y$, also the coefficient b_0 vanishes. Indeed, then the exact solution takes the form $\theta(r, \phi) = \Phi_0(\phi)$ [32], and the absence of any radial dependence is evident in Fig. 1(c,d). For $\lambda_x = -\lambda_y \rightarrow 0$, this solution smoothly deforms into an “ordinary” XY vortex with $\Phi_0(\phi) = \phi$, which is in stark contrast to the isotropic case, where the transition from the linear

to the non-linear problem is highly non-analytic. Since turning on the non-linearity in a fully anisotropic system does not alter the *radial dependence* of the far field of a single vortex, we conclude that the interaction of vortices at large distances is not screened as in the isotropic case, and thus the ordered phase is indeed stable in the thermodynamic limit. It is an interesting open question how the logarithmic dependence of the vortex field (3) in the SA regime affects the interaction at asymptotic distances.

Electrodynamic duality and vortex interaction.—The vortex interaction can be calculated explicitly within a dual electrodynamic formalism [3, 15]. This calculation treats the non-linearity in Eq. (1) perturbatively and is valid up to a finite but exponentially large scale we determine below. The duality defines the electric field as $\mathbf{E} = -\hat{\mathbf{z}} \times \nabla\theta$. For the overdamped dynamics described by Eq. (1), fluctuations of the magnetic field are gapped and can be integrated out. The basic equations are then Gauss’ law $\nabla \cdot \mathbf{E} = 2\pi n/\varepsilon$, and

$$\varepsilon \partial_t \mathbf{E} = -D \nabla \times (\nabla \times \mathbf{E}) - 2\pi \mathbf{j} - \hat{\mathbf{z}} \times \nabla \left(\sum_{i=x,y} \frac{\lambda_i}{2} E_i^2 + \eta \right). \quad (5)$$

The dielectric constant ε accounts for screening of the electric field due to fluctuations consisting of bound vortex pairs. It takes the microscopic value $\varepsilon = 1$, and is renormalized upon coarse-graining as described below. n and \mathbf{j} are the vortex density and current, respectively, which obey the continuity equation $\partial_t n = -\nabla \cdot \mathbf{j}$. For $n = \mathbf{j} = 0$, Eq. (5) reduces to the non-compact anisotropic KPZ equation. The vortex density is controlled by the fugacity y . Close to the putative unbinding transition $y \ll 1$, and we restrict ourselves to consider a dipole, $n(\mathbf{r}) = \sum_{\sigma=\pm} \sigma \delta(\mathbf{r} - \mathbf{r}_\sigma)$, where $\sigma = \pm$ are the charges of the vortices. They are assumed to undergo diffusive motion [31, 33, 34] according to

$$\frac{d\mathbf{r}_\sigma}{dt} = \mu \sigma \mathbf{E}(\mathbf{r}_\sigma) + \boldsymbol{\xi}_\sigma, \quad (6)$$

and the correlations of the zero-mean Gaussian noise sources $\boldsymbol{\xi}_\sigma$ are given by $\langle \xi_{\sigma,i}(t) \xi_{\sigma',j}(t') \rangle = 2\mu T \delta_{\sigma\sigma'} \delta_{ij} \delta(t - t')$, where the vortex “temperature” T is related to the noise strength Δ in Eq. (1) [3]. The vortex mobility μ is introduced phenomenologically, and we consider the limit of low mobility $\mu \ll D$. Then, retardation effects due to the vortices’ motion are negligible, and $\mathbf{E}(\mathbf{r}_\sigma)$ in Eq. (6) can be approximated by the instantaneous electrostatic field which is determined by Eq. (5) with $\partial_t \mathbf{E} = \mathbf{j} = \eta = 0$ [3]. Details of this calculation are given in the Supplement [32], and here we only point out key features of the solution. To address the possibility of a bound state, we focus on the dynamics of the dipole moment $\mathbf{r} = \sum_{\sigma=\pm} \sigma \mathbf{r}_\sigma = \mathbf{r}_+ - \mathbf{r}_-$. We parametrize the non-linearity as $\alpha_\pm = (\lambda_x \pm \lambda_y)/(2D)$, with $\alpha_- = 0$ and $\alpha_+ = 0$ corresponding to isotropic and fully anisotropic systems, respectively. The “isotropic” second-order correction $\propto \alpha_\pm^2$ was obtained previously [3]. It is a cen-

tral, conservative, and, crucially, *repulsive* force. In the “anisotropic” second-order correction $\propto \alpha_-^2$, the leading contribution is also central and conservative, but *attractive*. Additionally, it features sub-leading terms that cannot be derived from a potential. The “mixed” correction $\propto \alpha_+ \alpha_-$ includes terms $\propto (x, -y)$ that favor alignment of the dipole along one of the principal axes, in line with numerical simulations of the anisotropic CGLE [35, 36].

The isotropic, anisotropic, and mixed corrections are power series in logarithms $\ln(r/a)$. Thus, perturbation theory breaks down at a scale $L_v \sim ae^{1/\alpha_{\max}}$ where $\alpha_{\max} = \max\{|\alpha_\pm|\}$. In weakly out-of-equilibrium (and thus weakly non-linear) systems, the scale L_v can easily be much larger than any experimentally relevant system size. Then, we expect the dynamics of vortices to be described by the perturbatively obtained interaction. In the following, we discuss how the usual KT theory is modified due to non-equilibrium conditions and anisotropy. We focus on the FA configuration, where anisotropy has the most profound impact. Moreover, and as discussed in detail in [32], a vast simplification occurs in the FA case on scales $r \ll L_T = ae^{(T/\alpha_{\max})^{1/3}}$: Then, fluctuations of the orientation of the dipole lead to an angular averaging, rendering the problem effectively isotropic. Strong anisotropy is nevertheless manifest in the result of the angular average.

Vortex unbinding crossover.—The noise in Eqs. (5) and (6) creates pairs of vortices and antivortices which then diffuse under the influence of their interaction and eventually recombine. Such fluctuations on short scales between the microscopic cutoff a and a running cutoff scale ae^ℓ renormalize the parameters that enter an effective description on larger scales. This is described by the following RG flow equations [32]:

$$\begin{aligned} \frac{d\varepsilon}{d\ell} &= \frac{2\pi^2 y^2}{T}, & \frac{dy}{d\ell} &= \frac{1}{2} \left(4 - \frac{1}{\varepsilon T} + \frac{c\alpha_-^2}{3\varepsilon^2} \right) y, \\ \frac{dT}{d\ell} &= \frac{c\alpha_-^2 T}{3\varepsilon^2}, & \frac{dc}{d\ell} &= -3, \end{aligned} \quad (7)$$

where c is the running coefficient of the term $\propto \ln(r/a)^2$ in the effective dipole distribution with microscopic value $c = 3/2$ (see [32]; recall that also the microscopic value $\varepsilon = 1$ is fixed). Integrating the flow equation for c yields $c = 3(1 - 2\ell)/2$, i.e., the logarithmic scale ℓ appears explicitly in the flow equations for the remaining couplings. This again necessarily invalidates the perturbative flow equations at large scales — however, the condition $r \ll L_v$, which we assumed in the derivation of the flow equations, is always more stringent. Note also that the characteristic KPZ scale on which the renormalization of the (suitably rescaled) non-linearity in Eq. (1) due to non-topological fluctuations becomes substantial, is generically much larger than L_v, L_T [3]. Hence, analyzing Eqs. (7) we can consider α_- as a fixed parameter.

The RG flow is shown in Fig. 2. Remarkably, it is qualitatively different from both the equilibrium KT flow and the RG flow in an isotropic non-equilibrium sys-

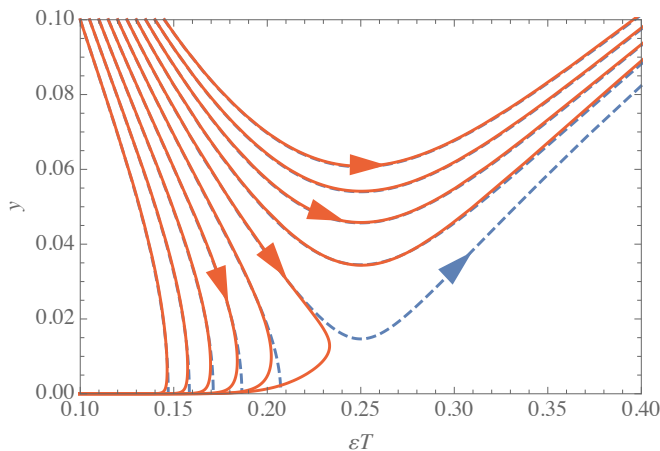


Figure 2. (Color online) RG flow (7). Dashed, blue: KT flow for $\alpha_-^2 = 0$; Solid, red: $\alpha_-^2 = 0.01$. There are two phases with $y, \varepsilon T \rightarrow 0$ ($\varepsilon T \rightarrow \text{const.}$ for $\alpha_-^2 = 0$) and $y, \varepsilon T \rightarrow \infty$, respectively. For $\alpha_-^2 = 0.01$, the critical temperature is $T_c \approx 0.13$, which is slightly larger than the KT critical temperature. The microscopic value of the fugacity is chosen as $y = 0.1$, and the temperature is varied in the range $T = 0.1, \dots, 0.145$.

tem. The most striking feature is the existence of a low-temperature phase in which vortices remain bound and fluctuations are anomalously suppressed since both $y, T \rightarrow 0$. In contrast, in isotropic systems vortices unbind at any finite temperature [3]; the low-temperature ordered phase in thermal equilibrium, on the other hand, is different in that T is conserved by the RG flow. The strong suppression of vortex fluctuations can be traced back to the dominant correction to the vortex interaction being *attractive* in the FA case. Consequently, the fundamental difference to the flow equations for isotropic systems in Ref. [3] is that here c flows to *negative* values, and therefore the terms $\propto c$ in the equations for T and y renormalize these quantities to *lower* values, thus antagonizing the unbinding of vortices. This leads to *increased* stability of the ordered phase as compared to the equilibrium case: The critical temperature T_c is higher for the same value of y . Heuristically, the lower the probability for vortex pairs to be created at a microscopic scale, the stronger noise-induced fluctuations the system can afford and still remain ordered. This is true also in equilibrium, but here we found that for $y \rightarrow 0$ the critical temperature *diverges* whereas it remains finite in KT theory.

While at low temperatures the flow $T \rightarrow 0$ is presumably cut at large scales when the flow equations (7) become invalid, at high temperatures the rapid growth of ε , indicating the screening of vortex interactions, stops the flow of T . Then, at larger scales, the flow in the disordered phase is the same as in equilibrium [32] (in particular, $y, \varepsilon \rightarrow \infty$).

The existence of two distinct phases points to the existence of a fixed point that controls critical behavior at the transition. Even if the “true” critical behavior at the largest scales is not captured by the flow equations (7),

they still entail the finite-size criticality that is observable up to parametrically large scales. However, in contrast to usual continuous phase transitions, the flow equations (7) cannot have a true fixed point since c grows steadily. A “flowing fixed point” can be found by the change of variables $\tilde{\varepsilon} = \varepsilon/x$, $\tilde{y} = \sqrt{xy}$, and $\tilde{T} = xT$, where $x = -c$ (note that $c < 0$ in the regime of interest at large ℓ), which recasts the flow equations as

$$\begin{aligned} \frac{d\tilde{\varepsilon}}{dx} &= \frac{1}{x} \left(\frac{2\pi^2 \tilde{y}^2}{3\tilde{T}} - \tilde{\varepsilon} \right), & \frac{d\tilde{T}}{dx} &= \frac{1}{3x} \left(3 - \frac{\alpha_-^2}{3\tilde{\varepsilon}^2} \right) \tilde{T}, \\ \frac{d\tilde{y}}{dx} &= \frac{1}{6} \left[4 - \frac{1}{\tilde{\varepsilon}\tilde{T}} + \frac{1}{x} \left(3 - \frac{\alpha_-^2}{3\tilde{\varepsilon}^2} \right) \right] \tilde{y}. \end{aligned} \quad (8)$$

These equations have a fixed point at $\tilde{\varepsilon}_* = |\alpha_-|/3$, $\tilde{y}_* = \sqrt{3/8}(1/\pi)$, $\tilde{T}_* = 3/(4|\alpha_-|)$. The existence of this fixed point implies that the correlation length diverges at the transition: As T is tuned closer to its critical value, the RG flow stays close to the fixed point up to larger scales before it eventually runs off to the ordered or disordered phase. In the disordered high-temperature phase, the correlation length is given by the scale at which the flow trajectory departing from the vicinity of the fixed point reaches $y = 1$. It can be calculated from an asymptotic analysis of the linearized flow equations, which yields [32]

$$4\sqrt{\ln(\xi/a)} + \ln(\ln(\xi/a))/4 \sim -\ln(t), \quad (9)$$

where $t = (T - T_c)/T_c$ is the reduced temperature. This peculiar universal divergence of ξ is stronger than conventional scaling $\xi/a \sim t^{-\nu}$ but weaker than the essential singularity $\xi/a \sim e^{C/\sqrt{t}}$ at the equilibrium KT transition. Experimentally or numerically, it will be challenging to confirm the precise type of singularity (9) — especially, since the asymptotic seems to be approached only for T very close to T_c when ξ becomes extremely large [32]. A more easily accessible feature that distinguishes the transition is the absence of the characteristic jump of the superfluid stiffness $\sim 1/\varepsilon$ with the universal value $1/(\varepsilon T) \rightarrow 4$ for T approaching T_c from below in the KT transition. Here, in contrast, the renormalized value of ε diverges at T_c , leading to a smoothly vanishing superfluid stiffness at the transition.

Conclusions.—We studied the effect of strong spatial anisotropy on the structure and dynamics of vortices in 2D out-of-equilibrium systems with U(1) symmetry. These are described by the caKPZ equation (1), and physical realizations include active systems [11], driven-dissipative condensates [3, 8–10, 12–18], oscillator arrays [20], and limit-cycle phases [21–25]. To address the thermodynamic stability of the ordered phase in which vortices exist only as tightly bound pairs, we considered the structure of single vortices. The absence of a radially emitted wave in the FA configuration indicates that the interaction is long-range and thus the ordered phase could be stable. Our perturbative calculation of the vortex interaction shows that in FA and up to an exponentially large scale, the vortex dynamics is dom-

inated by Coulomb interactions with *attractive* corrections. Consequently, the characteristic KT behavior such as an essential singularity of the correlation length and an universal jump (rounded by finite size) of the superfluid density gives way to novel universal behavior. This prediction could be checked directly in experiments (e.g., with exciton-polaritons, see [18] for relevant parameter regimes) or numerics [37]. The modification of the vortex interaction should also have directly observable effects on phase-ordering kinetics [38–41], which is an

interesting problem for further studies. Another interesting question is whether the dynamical instability reported in Refs. [16, 20] and that would lead to explosive desynchronization in arrays of limit-cycle oscillators could be mitigated by going to the SA regime. Moreover, here we focused on the FA configuration. The extension of our analysis to arbitrary anisotropy is an open problem.

We thank I. Carusotto, S. Diehl, S. Gazit, L. He, A. Kamenev, M. Szymańska, G. Wachtel, and A. Zamora for helpful discussions, and we acknowledge funding through the ERC synergy grant UQUAM.

-
- [1] Igor Aranson and Lorenz Kramer, “The world of the complex Ginzburg-Landau equation,” *Rev. Mod. Phys.* **74**, 99–143 (2002).
- [2] Igor S. Aranson, Stefan Scheidl, and Valerii M. Vinokur, “Nonequilibrium dislocation dynamics and instability of driven vortex lattices in two dimensions,” *Phys. Rev. B* **58**, 14541–14547 (1998).
- [3] G. Wachtel, L. M. Sieberer, S. Diehl, and E. Altman, “Electrodynamical duality and vortex unbinding in driven-dissipative condensates,” *Phys. Rev. B* **94**, 104520 (2016).
- [4] G. Grinstein, David Mukamel, R. Seidin, and Charles Bennett, “Temporally periodic phases and kinetic roughening,” *Phys. Rev. Lett.* **70**, 3607–3610 (1993).
- [5] G. Grinstein, C. Jayaprakash, and R. Pandit, “Conjectures about phase turbulence in the complex Ginzburg-Landau equation,” *Phys. D Nonlinear Phenom.* **90**, 96–106 (1996).
- [6] L. M. Sieberer, S. D. Huber, E. Altman, and S. Diehl, “Dynamical Critical Phenomena in Driven-Dissipative Systems,” *Phys. Rev. Lett.* **110**, 195301 (2013), [arXiv:1301.5854](https://arxiv.org/abs/1301.5854).
- [7] L. M. Sieberer, S. D. Huber, E. Altman, and S. Diehl, “Nonequilibrium functional renormalization for driven-dissipative Bose-Einstein condensation,” *Phys. Rev. B* **89**, 134310 (2014).
- [8] Ehud Altman, Lukas M. Sieberer, Leiming Chen, Sebastian Diehl, and John Toner, “Two-Dimensional Superfluidity of Exciton Polaritons Requires Strong Anisotropy,” *Phys. Rev. X* **5**, 011017 (2015).
- [9] J. Keeling, L. M. Sieberer, E. Altman, L. Chen, S. Diehl, and J. Toner, “Superfluidity and Phase Correlations of Driven Dissipative Condensates,” (Cambridge University Press, Cambridge, 2016) 1st ed., p. 27, [arXiv:1601.04495](https://arxiv.org/abs/1601.04495).
- [10] L M Sieberer, M Buchhold, and S Diehl, “Keldysh field theory for driven open quantum systems.” *Rep. Prog. Phys.* **79**, 096001 (2016).
- [11] Leiming Chen and John Toner, “Universality for Moving Stripes: A Hydrodynamic Theory of Polar Active Smectics,” *Phys. Rev. Lett.* **111**, 088701 (2013).
- [12] Vladimir N. Gladilin, Kai Ji, and Michiel Wouters, “Spatial coherence of weakly interacting one-dimensional nonequilibrium bosonic quantum fluids,” *Phys. Rev. A* **90**, 023615 (2014).
- [13] Kai Ji, Vladimir N. Gladilin, and Michiel Wouters, “Temporal coherence of one-dimensional nonequilibrium quantum fluids,” *Phys. Rev. B* **91**, 045301 (2015).
- [14] Liang He, Lukas M. Sieberer, Ehud Altman, and Sebastian Diehl, “Scaling properties of one-dimensional driven-dissipative condensates,” *Phys. Rev. B* **92**, 155307 (2015).
- [15] L. M. Sieberer, G. Wachtel, E. Altman, and S. Diehl, “Lattice duality for the compact Kardar-Parisi-Zhang equation,” *Phys. Rev. B* **94**, 104521 (2016).
- [16] Liang He, Lukas M. Sieberer, and Sebastian Diehl, “Space-Time Vortex Driven Crossover and Vortex Turbulence Phase Transition in One-Dimensional Driven Open Condensates,” *Phys. Rev. Lett.* **118**, 085301 (2017).
- [17] Liang He and Sebastian Diehl, “Miscible-Immiscible Transition and Nonequilibrium Scaling in Two-Component Driven Open Condensate Wires,” (2017), [arXiv:1706.01373](https://arxiv.org/abs/1706.01373).
- [18] A. Zamora, L. M. Sieberer, K. Dunnett, S. Diehl, and M. H. Szymańska, “Tuning across universalities with a driven open condensate,” *Phys. Rev. X* **7** (2017), [10.1103/PhysRevX.7.041006](https://arxiv.org/abs/10.1103/PhysRevX.7.041006), [arXiv:1704.06609](https://arxiv.org/abs/1704.06609).
- [19] Davide Squizzato, Léonie Canet, and Anna Minguzzi, “Kardar-Parisi-Zhang universality in the phase distributions of one-dimensional exciton-polaritons,” (2017), [arXiv:1712.03709](https://arxiv.org/abs/1712.03709).
- [20] Roland Lauter, Aditi Mitra, and Florian Marquardt, “From Kardar-Parisi-Zhang scaling to explosive desynchronization in arrays of limit-cycle oscillators,” *Phys. Rev. X* **9**, 011001 (2016), [arXiv:1607.03696](https://arxiv.org/abs/1607.03696).
- [21] Tony E. Lee, H. Häffner, and M. C. Cross, “Antiferromagnetic phase transition in a nonequilibrium lattice of Rydberg atoms,” *Phys. Rev. A* **84**, 031402 (2011).
- [22] Max Ludwig and Florian Marquardt, “Quantum many-body dynamics in optomechanical arrays.” *Phys. Rev. Lett.* **111**, 073603 (2013).
- [23] Jiasen Jin, Davide Rossini, Rosario Fazio, Martin Leib, and Michael J Hartmann, “Photon solid phases in driven arrays of nonlinearly coupled cavities.” *Phys. Rev. Lett.* **110**, 163605 (2013).
- [24] Ching-Kit Chan, Tony E. Lee, and Sarang Gopalakrishnan, “Limit-cycle phase in driven-dissipative spin systems,” *Phys. Rev. A* **91**, 051601 (2015).
- [25] M. Schiró, C. Joshi, M. Bordyuh, R. Fazio, J. Keeling, and H. E. Türeci, “Exotic Attractors of the Nonequilibrium Rabi-Hubbard Model,” *Phys. Rev. Lett.* **116**, 143603 (2016).
- [26] Norman Y. Yao, Chetan Nayak, Leon Balents, and Michael P. Zaletel, “Classical Discrete Time Crystals,”

- (2018), [arXiv:1801.02628](https://arxiv.org/abs/1801.02628).
- [27] Dietrich Wolf, “Kinetic roughening of vicinal surfaces,” *Phys. Rev. Lett.* **67**, 1783–1786 (1991).
- [28] H. Sakaguchi and Y. Kuramoto, “A Soluble Active Rotator Model Showing Phase Transitions via Mutual Entertainment,” *Prog. Theor. Phys.* **76**, 576–581 (1986).
- [29] Juan A. Acebrón, L. L. Bonilla, Conrad J Pérez Vicente, Félix Ritort, and Renato Spigler, “The Kuramoto model: A simple paradigm for synchronization phenomena,” *Rev. Mod. Phys.* **77**, 137–185 (2005), [arXiv:0306625 \[cond-mat\]](https://arxiv.org/abs/0306625).
- [30] Then, the stationary distribution of the field θ is given by the Gibbs weight $\mathcal{P} \sim e^{-\mathcal{H}_{XY}}$ with $\mathcal{H}_{XY} = \frac{D}{\Lambda} \int d^2\mathbf{r} (\nabla\theta)^2$, and the usual equilibrium KT theory applies.
- [31] Igor S. Aranson, Hugues Chaté, and Lei-Han Tang, “Spiral Motion in a Noisy Complex Ginzburg-Landau Equation,” *Phys. Rev. Lett.* **80**, 2646–2649 (1998).
- [32] See Supplemental Material for details on the numerics and analytics for single vortices as well as the perturbative calculation of the vortex interaction, and the derivation and asymptotic analysis of the RG equations.
- [33] Vinay Ambegaokar, B. Halperin, David Nelson, and Eric Siggia, “Dissipation in Two-Dimensional Superfluids,” *Phys. Rev. Lett.* **40**, 783–786 (1978).
- [34] Vinay Ambegaokar, B. Halperin, David Nelson, and Eric Siggia, “Dynamics of superfluid films,” *Phys. Rev. B* **21**, 1806–1826 (1980).
- [35] Roland Faller and Lorenz Kramer, “Phase chaos in the anisotropic complex Ginzburg-Landau equation,” *Phys. Rev. E* **57**, R6249–R6252 (1998).
- [36] Roland Faller and Lorenz Kramer, “Ordered Defect Chains in the 2D Anisotropic Complex Ginzburg-Landau Equation,” *Chaos, Solitons & Fractals* **10**, 745–752 (1999).
- [37] Vladimir Gladilin and Michiel Wouters, “Interaction and motion of vortices in nonequilibrium quantum fluids,” *New J. Phys.* (2017), [10.1088/1367-2630/AA83A1](https://doi.org/10.1088/1367-2630/AA83A1).
- [38] G. Ryskin and M. Kremenetsky, “Drag force on a line defect moving through an otherwise undisturbed field: Disclination line in a nematic liquid crystal,” *Phys. Rev. Lett.* **67**, 1574–1577 (1991).
- [39] B. Yurke, A. N. Pargellis, T. Kovacs, and D. A. Huse, “Coarsening dynamics of the XY model,” *Phys. Rev. E* **47**, 1525–1530 (1993).
- [40] A. J. Bray, A. J. Briant, and D. K. Jervis, “Breakdown of Scaling in the Nonequilibrium Critical Dynamics of the Two-Dimensional XY Model,” *Phys. Rev. Lett.* **84**, 1503–1506 (2000).
- [41] A. J. Bray, “Random walks in logarithmic and power-law potentials, nonuniversal persistence, and vortex dynamics in the two-dimensional XY model,” *Phys. Rev. E - Stat. Physics, Plasmas, Fluids, Relat. Interdiscip. Top.* **62**, 103–112 (2000), [arXiv:9910135 \[cond-mat\]](https://arxiv.org/abs/9910135).

Supplemental Material: Topological Defects in Anisotropic Driven Open Systems

In the Supplemental Material, we present details of our analysis of single-vortex solutions in the compact anisotropic KPZ equation. We study these solutions using asymptotic analysis and numerics. Moreover, we calculate the interaction between a vortex and an antivortex in the limit of low mobility of topological defects. In this limit, the interaction can be obtained from a dual electrostatic description. We solve the electrostatic problem perturbatively in the non-linearity of the KPZ equation. Based on this calculation, we derive RG equations that describe the vortex-unbinding crossover in parametrically large systems. Our analysis of the critical RG flow trajectories reveals a peculiar universal divergence of the correlation length as the transition is approached from the disordered side.

CONTENTS

I. A single vortex in the compact anisotropic KPZ equation	1
A. Far field of a single anisotropic vortex	2
B. Numerics	4
II. Interaction of vortices in the compact anisotropic KPZ equation	4
A. Electrodynamical duality	4
B. Perturbative calculation of the vortex interaction	6
1. First order correction	8
2. Second order correction: diagonal terms	9
3. Second order correction: mixed terms	12
4. Numerical checks	14
III. Dynamics of vortices in the compact anisotropic KPZ equation	15
A. Equations of motion	15
B. Stationary distribution of a dipole	19
IV. RG flow	19
A. Derivation of the RG flow equations	19
B. Phases and fixed point of the RG flow	22
C. Asymptotic analysis of the linearized flow equations	23

I. A SINGLE VORTEX IN THE COMPACT ANISOTROPIC KPZ EQUATION

Here we present some details of our analysis of the field generated by a single topological defect in the compact anisotropic KPZ (caKPZ) equation. As explained in the main text, to judge whether the ordered phase is stable in the thermodynamic limit, the crucial question is how the interaction of vortices behaves at asymptotically large distances. This question cannot be addressed within the perturbative treatment of the non-linearity we formulate below in the framework of the electrodynamic duality, since the perturbative expansion breaks down at large distances. We can nevertheless gain some insight by considering the simpler problem of a single vortex: In the isotropic KPZ equation, these vortices emit waves in the radial direction, and the exponential screening of the vortex interaction can be traced back to the shocks

which are created when the emitted waves collide. Thus — at least heuristically — we conclude that the interaction is not screened if there are no waves emitted from the vortex cores in the (strongly) anisotropic KPZ equation. (Recall that due to the non-linearity a multi-vortex solution cannot simply be constructed by linear superposition of single vortices.) Below, using a combination of analytical asymptotic analysis and numerics we show that this is indeed the case in the fully anisotropic KPZ equation. We find that in the full weakly anisotropic (WA) regime, topological defects emit (deformed) radial waves and we would expect their interactions to be exponentially screened. Radial waves correspond to the asymptotic behavior $\theta(r, \phi) \sim k_0(\phi)r$ for $r \rightarrow \infty$ of the field generated by a topological defect at the origin, where $k_0(\phi)$ is the asymptotic wave number that depends on the polar angle ϕ . By contrast, in the strongly anisotropic (SA) regime, the leading asymptotic behavior of the far-field of a topological defect is $\theta(r, \phi) \sim b_0 \ln(r/a) + \Phi(\phi)$, and the coefficient b_0 vanishes at the fully anisotropic (FA) point ($\lambda_x = -\lambda_y$). Thus, vortices in the fully anisotropic KPZ equation are qualitatively very similar to ordinary vortices in the XY model. Away from the fully anisotropic point, the asymptotics $\theta(r, \phi) \sim b_0 \ln(r/a)$ can be interpreted as a radial wave with a wave number that vanishes as $1/r$. Further studies are required to test whether this behavior leads to sufficient screening to destabilize the ordered phase.

We thus want to find solutions to the caKPZ equation without noise,

$$\partial_t \theta = D \nabla^2 \theta + \frac{\lambda_x}{2} (\partial_x \theta)^2 + \frac{\lambda_y}{2} (\partial_y \theta)^2, \quad (1)$$

subject to the topological constraint $\oint d\mathbf{l} \cdot \nabla \theta = 2\pi$, where the line integral encircles the vortex core. As we show below, in the WA regime, such vortex solutions oscillate uniformly, i.e., they take the form $\theta(\mathbf{r}, t) = \theta_0(\mathbf{r}) + \omega_0 t$, where $\omega_0 > 0$ for $\lambda_{x,y} > 0$. We thus find it convenient to rewrite Eq. (1) in a rotating frame by the transformation $\theta \rightarrow \theta - \omega_0 t$, such that

$$\partial_t \theta = D \nabla^2 \theta + \frac{\lambda_x}{2} (\partial_x \theta)^2 + \frac{\lambda_y}{2} (\partial_y \theta)^2 - \omega_0 = 0, \quad (2)$$

which is the equation stated in the main text [Eq. (2)]. This is a non-linear partial differential equation, and in the absence of rotational symmetry, the solution cannot

be separated into parts that depend only on the radial coordinate or polar angle, respectively. As a further complication, the continuum compact KPZ (cKPZ) equation has to be regularized at short distances (e.g., by considering the cKPZ equation as the far-field phase equation derived from the complex Ginzburg-Landau equation (CGLE), or by discretizing the cKPZ equation on a lattice). In particular, the value of the oscillation frequency is determined by the regularization. Nevertheless, some progress can be made if we are modest and consider the asymptotic far-field behavior only. Below, we check our analytical results for the far field with numerics for the full solution of Eq. (1).

We begin the discussion of the analytical approach by reviewing vortices in the isotropic KPZ equation [?] (see [?] and references therein for vortices in the CGLE). Hence, we set $\lambda_x = \lambda_y = \lambda_+$ in Eq. (2),

$$\partial_t \theta = D \nabla^2 \theta + \frac{\lambda_+}{2} (\nabla \theta) - \omega_0 = 0. \quad (3)$$

A vortex sitting at the origin is described by a solution of the form $\theta(r, \phi) = \phi + R(r)$, where due to the rotational symmetry the function $R(r)$ depends only on the radius. For the radial dependence we find the equation ($\alpha_+ = \lambda_+/(2D)$)

$$\left(R'' + \frac{R'}{r} \right) + \alpha_+ \left[\frac{1}{r^2} + R'^2 \right] - \frac{\omega_0}{D} = 0, \quad (4)$$

which can be linearized by means of a Cole-Hopf transformation, $w = e^{\alpha_+ R}$. We note that this implies that w takes values in $\mathbb{R}_{>0}$ since $R \in \mathbb{R}$. The Cole-Hopf transformation brings Eq. (4) to the form of a modified Bessel equation,

$$w'' + \frac{w'}{r} + \frac{\alpha_+^2 w}{r^2} = \kappa_0^2 w, \quad (5)$$

where $\kappa_0^2 = \alpha_+ \omega_0 / D$. For $\omega_0 = 0$, two linearly independent solutions to this equation are given by $w = r^{\pm i \alpha_+}$, and accordingly real-valued solutions take the form $w = w_0 \cos(\alpha_+ \ln(r/a) + b)$ with $w_0, b \in \mathbb{R}$. However, this oscillating function does not have an inverse Cole-Hopf transformation $\forall r \in \mathbb{R}_{>0}$ and thus it does not yield a valid solution for a vortex. For finite ω_0 , the solution to Eq. (5) which is bounded at large r is the modified Bessel function $w(r) = K_{i \alpha_+}(\kappa_0 r)$. At large scales it behaves as $w(r) \sim e^{-\kappa_0 r} / \sqrt{r}$ and it assumes a maximum at $r_0 = e^{-\pi/(2\alpha_+)}/\kappa_0$, while at shorter scales it starts to oscillate. Hence, the KPZ equation can describe vortices only for $r > r_0$, and some regularization is required at shorter scales. The precise value of ω_0 is determined by the regularization [?]. In the CGLE, one finds $\omega_0 \sim \lambda_+ e^{-\pi D/\lambda_+}/(2a)$, where a is the vortex core radius [?]. Before we move on to discuss vortices in the anisotropic case, we note that the asymptotic behavior of the Bessel function implies the following asymptotic

behavior of θ :

$$\begin{aligned} \theta(r, \phi) &= \phi + \frac{1}{\alpha_+} \ln(K_{i \alpha_+}(\kappa_0 r)) \\ &= -k_0 r - \frac{1}{2\alpha_+} \ln(2\alpha_+ \kappa_0 r / \pi) + \phi + O(1/r), \end{aligned} \quad (6)$$

where $k_0 = \kappa_0 / \alpha_+ = \sqrt{\omega_0 / (\alpha_+ D)}$.

A. Far field of a single anisotropic vortex

Next, we consider vortices in the anisotropic KPZ equation, i.e., we seek solutions to

$$\nabla^2 \theta + \alpha_x (\partial_x \theta)^2 + \alpha_y (\partial_y \theta)^2 - \varpi_0 = 0, \quad (7)$$

where $\varpi_0 = \omega_0 / D$, $\alpha_{x,y} = \lambda_{x,y} / (2D)$, and with $\alpha_x \neq \alpha_y$. The asymptotic behavior in the isotropic case (6) motivates the following ansatz for $r \rightarrow \infty$:

$$\theta(r, \phi) = k_0(\phi) r + b(\phi) \ln(r/a) + \Phi(\phi) + O(1/r). \quad (8)$$

Here, $\Phi(\phi)$ contains the topological part, i.e., $\int_0^{2\pi} d\phi \Phi'(\phi) = 2\pi$, where $\Phi' = d\Phi/d\phi$. We note, that a constant contribution to the vortex field can be added arbitrarily. It is not determined by the cKPZ equation, since the latter contains only derivatives of θ . With the above ansatz, the gradient of the phase behaves at large r as

$$\begin{aligned} \nabla \theta(r, \phi) &= \hat{\mathbf{e}}_r \left(k_0(\phi) + \frac{b(\phi)}{r} \right) \\ &+ \frac{\hat{\mathbf{e}}_\phi}{r} (k_0'(\phi) r + b'(\phi) \ln(r/a) + \Phi'(\phi)) + O(1/r^2), \end{aligned} \quad (9)$$

where $\hat{\mathbf{e}}_r = (\cos(\phi), \sin(\phi))$, and $\hat{\mathbf{e}}_\phi = (-\sin(\phi), \cos(\phi))$. Inserting this expression in Eq. (7), we find by matching the leading terms for $r \rightarrow \infty$ (for $\alpha_{x,y} > 0$, we take the negative square root to match our numerical findings, see Sec. IB; $k(\phi)$ is positive for $\alpha_{x,y} < 0$):

$$k_0(\phi) = -\sqrt{\frac{\varpi_0}{\alpha_x \cos(\phi)^2 + \alpha_y \sin(\phi)^2}}, \quad (10)$$

which describes a vortex emitting a slightly deformed radial wave. Clearly, this solution is well-behaved as a function of ϕ as long as both α_x and α_y are positive. As in the isotropic case, we expect that ϖ_0 is determined by matching the asymptotic solution to the (regularized) solution in the core region. However, we cannot perform a Cole-Hopf transformation as before, and therefore it is not easily possible to find a solution that is valid at short distances. Crucially, within the WA regime, the structure of a single vortex is qualitatively unchanged, which implies that the vortex interaction is screened and the ordered phase is unstable whenever $\alpha_{x,y}$ have the same sign.

In the SA regime, when α_x and α_y have opposite signs, Eq. (10) indicates that ϖ_0 and $k_0(\phi)$ vanish — any non-zero ϖ_0 would lead to imaginary values of $k_0(\phi)$ and can be discarded for this reason. This matches our numerical findings, see Sec. IB. Dropping the leading term from Eq. (8), we find by matching terms $O((\ln(r/a)/r)^2)$ in Eq. (7):

$$(\alpha_+ - \alpha_- \cos(2\phi)) b'(\phi)^2 = 0, \quad (11)$$

where $\alpha_{\pm} = (\alpha_x \pm \alpha_y)/2$. It follows that $b'(\phi) = 0$ and hence $b(\phi) = b_0$. All terms at $O(\ln(r/a)/r^2)$ vanish for $b'(\phi) = 0$, and the next non-trivial contribution comes at $O(1/r^2)$:

$$\begin{aligned} \Phi''(\phi) + \alpha_+ (b_0^2 + \Phi'(\phi)^2) + \alpha_- (b_0^2 \cos(2\phi) \\ - 2b_0\Phi'(\phi) \sin(2\phi) - \Phi'(\phi)^2 \cos(2\phi)) = 0. \end{aligned} \quad (12)$$

This is an ordinary yet non-linear differential equation, and there is no constructive way to find a solution. However, a vast simplification occurs in the FA limit $\alpha_x = -\alpha_y$. There, the numerical solution shown in Fig. 1 of the main text indicates that $\theta(r, \phi)$ does not depend on r at all, i.e., the ansatz $\theta(r, \phi) = \Phi_0(\phi)$ yields an exact solution. Going back to Eq. (2), with this ansatz we find

$$\begin{aligned} \nabla^2\theta + \alpha_- \left[(\partial_x\theta)^2 - (\partial_x\theta)^2 \right] \\ = \frac{1}{r^2} (\Phi_0'' - \alpha_- \cos(2\phi)\Phi_0'^2) = 0, \end{aligned} \quad (13)$$

This equation can be integrated trivially once,

$$\begin{aligned} \int_0^\phi d\phi' \frac{\Phi_0''(\phi')}{\Phi_0'(\phi')^2} &= - \int_0^\phi d\phi' \frac{d}{d\phi'} \frac{1}{\Phi_0'(\phi')} \\ &= - \left(\frac{1}{\Phi_0'(\phi)} - \frac{1}{\Phi_0'(0)} \right) \\ &= \alpha_- \int_0^\phi d\phi' \cos(2\phi') \\ &= \frac{\alpha_-}{2} \sin(2\phi). \end{aligned} \quad (14)$$

We thus find

$$\Phi_0'(\phi) = \frac{\Phi_0'(0)}{1 - \frac{\alpha_-}{2} \Phi_0'(0) \sin(2\phi)}, \quad (15)$$

and another integration yields the result

$$\begin{aligned} \Phi_0(\phi) = 2\nu\Phi_0'(0) (\arctan(\nu(2\tan(\phi) - \alpha_-\Phi_0'(0))) \\ + \arctan(\alpha_-\nu\Phi_0'(0))), \end{aligned} \quad (16)$$

where a constant of integration is added such that $\Phi_0(0) = 0$; in order to obtain a smooth solution we have to choose different branches of the arctan in the intervals $0 < \phi < \pi/2$, $\pi/2 < \phi < 3\pi/2$, and $3\pi/2 < \phi < 2\pi$. The constant ν in Eq. (16) is given by

$$\nu = \frac{1}{\sqrt{4 - (\alpha_-\Phi_0'(0))^2}}. \quad (17)$$

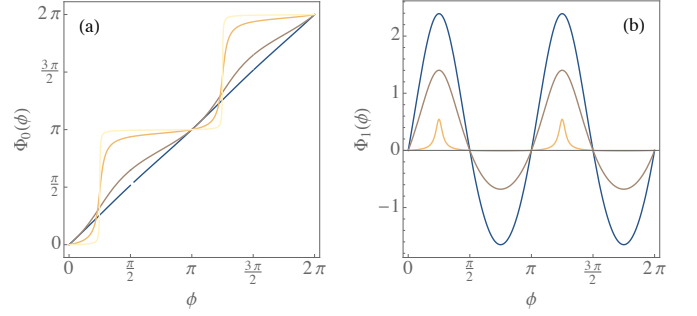


Figure 1. (a) Angular dependence of the vortex field in the fully anisotropic KPZ equation for $\alpha_- = 0.1, 1, 10, 100$ (blue to light orange). (b) First-order correction to the fully anisotropic vortex for $\alpha_- = 0.5, 1, 10$ (blue to orange).

Finally, $\Phi_0'(0)$ is determined by the condition that for a singly-charged vortex the function $\Phi_0(\phi)$ should wind once around the unit circle, which yields

$$\Phi_0'(0) = \frac{2}{\sqrt{4 + \alpha_-^2}}. \quad (18)$$

Vortex solutions for different values of α_- are shown in Fig. 1(a). For $\alpha_- \rightarrow 0$ the solution smoothly deforms into an “ordinary” XY-type vortex with $\Phi_0(\phi) = \phi$, while in the opposite limit it approaches a step-like form. In fact, Eq. (16) is analytic in α_- at $\alpha_- = 0$. This is in stark contrast to the isotropic case, where the transition from the linear to the non-linear problem is highly non-analytic (see the above expression for ω_0). Since turning on the non-linearity in a fully anisotropic system does not alter the *radial dependence* of the far field of a single vortex, we conclude that the interaction of vortices at large distances is not screened as in the isotropic case, and thus the ordered phase can be stable.

Now let’s reinstate α_+ . First, note that for $b_0 = 0$, Eq. (12) becomes

$$\Phi''(\phi) + (\alpha_+ - \alpha_- \cos(2\phi)) \Phi'(\phi)^2 = 0. \quad (19)$$

As before, this equation can be integrated and we find

$$- \left(\frac{1}{\Phi'(\phi)} - \frac{1}{\Phi'(0)} \right) = -\alpha_+\phi + \frac{\alpha_-}{2} \sin(2\phi). \quad (20)$$

Since the resulting expression for $\Phi'(\phi)$ is not periodic in ϕ , evidently this cannot be a valid solution, and we have to allow for a finite value of b_0 , i.e., away from the FA configuration vortices do have a non-trivial radial dependence. We restrict ourselves to small values of α_+ for which we set

$$\begin{aligned} \Phi(\phi) = \Phi_0(\phi) + \alpha_+\Phi_1(\phi) + O(\alpha_+^2), \\ b_0 = \alpha_+b_{01} + O(\alpha_+^2), \end{aligned} \quad (21)$$

where the zeroth-order solution $\Phi_0(\phi)$ is given by Eq. (16). Inserting this ansatz in Eq. (12) leads to a linear

second-order differential equation for $\Phi_1(\phi)$; b_{01} is determined by the condition that $\Phi'_0(\phi)$ has to be periodic, which yields $b_{01} = -2/\alpha_-^2$. The first constant of integration $\Phi'_1(0)$ has to be chosen such that $\lim_{\phi \searrow 0} \Phi_1(\phi) = \lim_{\phi \nearrow 2\pi} \Phi_1(\phi)$, while w.l.o.g. we choose the second constant of integration $\Phi_1(0)$ such that $\Phi(0) = 0$. The resulting solution $\Phi_1(\phi)$ is shown in Fig. 1(b). It is an interesting question for future research how the logarithmic dependence of the vortex field (8) on the distance from the core — corresponding to an emitted wave with wave number $\sim 1/r$ — affects the interaction at asymptotic distances.

B. Numerics

To confirm the results of the previous section numerically, we discretize Eq. (1) on a lattice with sites $\mathbf{r} = (x, y)$, i.e., we replace spatial derivatives with finite differences according to (cf. Ref. [? ?])

$$\begin{aligned} \partial_x^2 \theta &\rightarrow - \sum_{\sigma=\pm} \sin(\theta_{\mathbf{r}} - \theta_{\mathbf{r}+\sigma\hat{\mathbf{x}}}), \\ (\partial_x \theta)^2 &\rightarrow - \sum_{\sigma=\pm} (\cos(\theta_{\mathbf{r}} - \theta_{\mathbf{r}+\sigma\hat{\mathbf{x}}}) - 1). \end{aligned} \quad (22)$$

$\hat{\mathbf{x}}$ and $\hat{\mathbf{y}}$ are unit vectors, and for convenience we choose the lattice spacing as $a = 1$. With the above prescription, Eq. (1) becomes

$$\begin{aligned} \partial_t \theta_{\mathbf{r}} = - \sum_{\sigma=\pm} &\left[D (\sin(\theta_{\mathbf{r}} - \theta_{\mathbf{r}+\sigma\hat{\mathbf{x}}}) + \sin(\theta_{\mathbf{r}} - \theta_{\mathbf{r}+\sigma\hat{\mathbf{y}}})) \right. \\ &+ \frac{\lambda_x}{2} (\cos(\theta_{\mathbf{r}} - \theta_{\mathbf{r}+\sigma\hat{\mathbf{x}}}) - 1) \\ &\left. + \frac{\lambda_y}{2} (\cos(\theta_{\mathbf{r}} - \theta_{\mathbf{r}+\sigma\hat{\mathbf{y}}}) - 1) \right]. \end{aligned} \quad (23)$$

We choose initial conditions corresponding to an ordinary XY vortex that is displaced by half a lattice spacing from the origin, i.e., $\theta_{\mathbf{r}}(0) = \tan((y-1/2)/(x-1/2))$, and evolve this configuration in time. For open boundary conditions, we found that the core of the topological defect remains stationary. (For large values of the nonlinearities $\lambda_{x,y}$, the vortex starts to move, and new vortices are generated dynamically. In the simulations presented here, we always stay below this instability.) Since the evolution equation (23) is dissipative and the topological charge is conserved, the field configuration converges to a vortex solution of the non-linear problem. For the plots in Fig. 1 of the main text, we evolved Eq. (23) on a lattice of 200×200 sites.

As discussed in the previous section, vortices in the caKPZ equation oscillate uniformly in the WA regime. From the numerical solution of Eq. (23), the oscillation frequency can be obtained by fitting the steady linear growth of $\theta_{\mathbf{r}}(t)$ at late times (i.e., when convergence is reached). We find a vanishing oscillation frequency ϖ_0

only exactly at the FA point, and small but finite oscillation frequencies throughout the SA region. However, as illustrated in Fig. 2, this is just a finite-size effect.

II. INTERACTION OF VORTICES IN THE COMPACT ANISOTROPIC KPZ EQUATION

In linear theories, the superposition of two solutions gives another valid solution. This is no longer true in the presence of a non-linearity as in the case of the caKPZ equation. In particular, the superposition of two single-vortex solutions does not yield a two-vortex solution. This is the main difficulty in trying to find the vortex interaction. Only for very large separations of topological defects, we could gain some insight in the asymptotic behavior of the vortex interaction as discussed in the previous section. Here, we present an alternative approach that works up to parametrically large distances, and is based on a recently developed formulation of the caKPZ equation as non-linear electrodynamics [? ?].

In Sec. II A, we briefly review the electrodynamic duality for the compact KPZ equation [? ?] and its extension to the anisotropic case. Within this framework, we calculate the interaction between a vortex and an antivortex perturbatively. This rather tedious calculation, and some numerical checks of the result, are presented in Sec. II B.

A. Electrodynamic duality

In the following, we derive a dual description of the caKPZ equation [Eq. (1) of the main text] [? ?],

$$\partial_t \theta = \sum_{i=x,y} \left[D_i \partial_i^2 \theta + \frac{\lambda_i}{2} (\partial_i \theta)^2 \right] + \eta. \quad (24)$$

As in the main text, we set $D_x = D_y = D$, which corresponds simply to an anisotropic rescaling of the units of length. We find it convenient to rewrite the non-linear terms in the following way:

$$\sum_{i=x,y} \lambda_i (\partial_i \theta)^2 = \lambda_+ (\nabla \theta)^2 + \lambda_- \left[(\partial_x \theta)^2 - (\partial_y \theta)^2 \right], \quad (25)$$

which separates an isotropic contribution that is proportional to $\lambda_+ = \frac{\lambda_x + \lambda_y}{2}$ from a purely anisotropic contribution with coefficient $\lambda_- = \frac{\lambda_x - \lambda_y}{2}$. To keep the notation compact, we define a \odot product of vectors $\mathbf{a} = (a_x, a_y)$ and $\mathbf{b} = (b_x, b_y)$ through the relation $\mathbf{a} \odot \mathbf{b} = a_x b_x - a_y b_y$. We also use the abbreviation $\mathbf{a}^{\odot 2} = \mathbf{a} \odot \mathbf{a} = a_x^2 - a_y^2$. It is straightforward to check that this product is commutative and distributive, i.e., in calculations it can be handled like the usual scalar product. With this notation, the caKPZ equation can be written as

$$\partial_t \theta = D \nabla^2 \theta + \frac{\lambda_+}{2} (\nabla \theta)^2 + \frac{\lambda_-}{2} (\nabla \theta)^{\odot 2} + \eta. \quad (26)$$

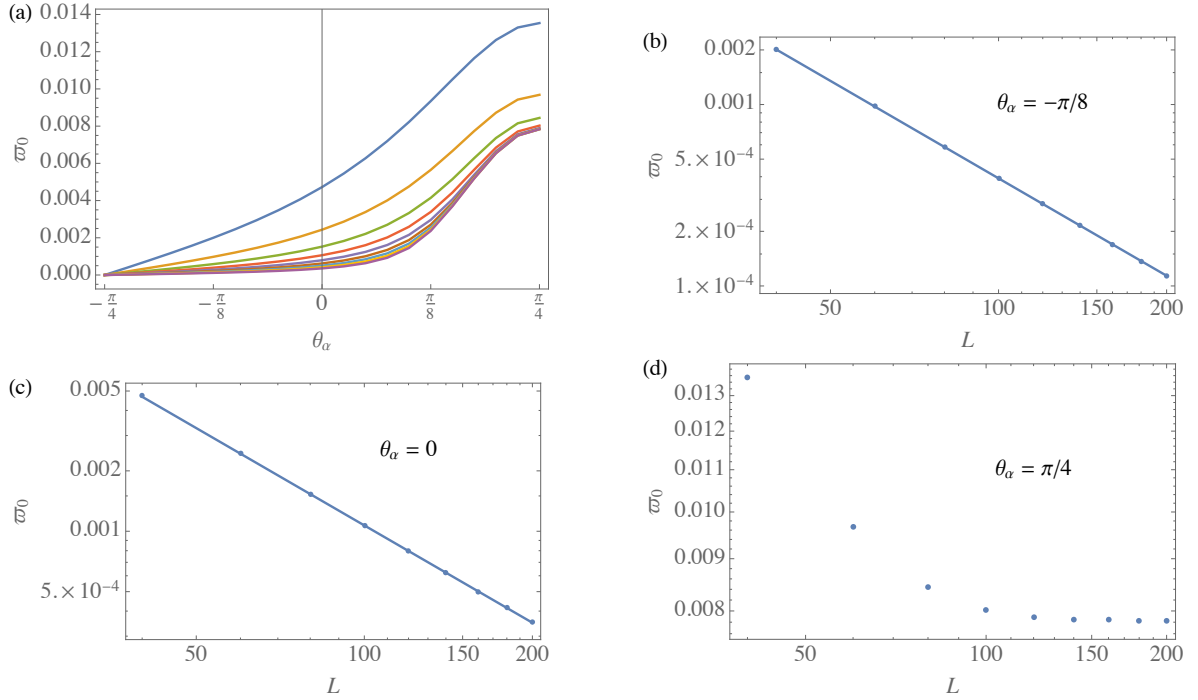


Figure 2. (a) Oscillation frequency $\varpi_0 = \omega_0/D$ as a function of θ_α . The latter is defined by $(\alpha_x, \alpha_y) = 1/2(\cos(\theta_\alpha), \sin(\theta_\alpha))$, i.e., for all values of θ_α the system is equally non-linear in the sense that $\sqrt{\alpha_x^2 + \alpha_y^2} = 1/2$, and only the degree of anisotropy is varied. Specifically, for $\theta_\alpha = -\pi/4$ the system is fully anisotropic; the separation between the SA and WA regimes is at $\theta_\alpha = 0$, and at $\theta_\alpha = \pi/4$ the system is isotropic. The different curves correspond to system sizes $L = 40, 60, 80, \dots, 200$ (top to bottom). Numerically, ϖ_0 vanishes only at the FA point, while it is finite due to finite-size effects everywhere else. (b,c) In the SA regime we found that ϖ_0 vanishes algebraically with increasing system size, while (d) it converges to a finite value in the isotropic case with $\theta_\alpha = \pi/4$ (and also for other values of θ_α in the WA regime).

To explicitly incorporate vortices in the caKPZ equation, we reformulate it in terms of the electric field, which is defined as

$$\mathbf{E} = -\hat{\mathbf{z}} \times \nabla\theta. \quad (27)$$

$\hat{\mathbf{z}} = (0, 0, 1)$ is a unit vector pointing in the direction perpendicular to the xy -plane on which θ and \mathbf{E} are defined. We note that in the presence of topological defects in the KPZ equation without noise, θ has a contribution that depends linearly on time and is uniform in space, see Sec. I. This contribution corresponds to oscillations of vortices in the complex Ginzburg-Landau equation, and drops out if we consider \mathbf{E} instead of θ .

By cyclic permutation of the vectors in the defining relation (27) for \mathbf{E} we obtain $\nabla\theta = \hat{\mathbf{z}} \times \mathbf{E}$, which leads to the following expressions for the non-linear terms in the caKPZ equation:

$$(\nabla\theta)^2 = E^2, \quad (\nabla\theta)^{\odot 2} = -\mathbf{E}^{\odot 2}. \quad (28)$$

Thus, Eq. (26) can be written as

$$\partial_t \mathbf{E} = D\nabla^2 \mathbf{E} - \hat{\mathbf{z}} \times \left(\frac{\lambda_+}{2} E^2 - \frac{\lambda_-}{2} \mathbf{E}^{\odot 2} + \eta \right). \quad (29)$$

This equation has to be extended to explicitly account for vortices. To this end, we first note that the circulation of

the gradient of θ around a closed loop is determined by the number of enclosed vortices. This statement, recast in differential form, can be written as

$$\nabla \cdot \mathbf{E} = 2\pi n, \quad (30)$$

where n is the vortex density. Second, since vortices are created only in pairs (or at the boundary of the sample), the vortex density n and current \mathbf{j} obey on equation of continuity:

$$\partial_t n + \nabla \cdot \mathbf{j} = 0. \quad (31)$$

Since Eqs. (30) and (31) can be combined to read

$$\nabla \cdot (\partial_t \mathbf{E} + 2\pi \mathbf{j}) = 0, \quad (32)$$

we see that

$$\partial_t \mathbf{E} = -2\pi \mathbf{j} + \nabla \times \mathbf{u}, \quad (33)$$

where \mathbf{u} is a vector field that is determined by the condition that Eq. (33) should reproduce the KPZ equation (29) in the absence of vortices, i.e., for $n = \mathbf{j} = 0$. This condition is fulfilled by setting

$$\mathbf{u} = -D\nabla \times \mathbf{E} + \hat{\mathbf{z}} \left(\frac{\lambda_+}{2} E^2 - \frac{\lambda_-}{2} \mathbf{E}^{\odot 2} + \eta \right). \quad (34)$$

The required extension of the KPZ equation (29) to include vortices is thus given by

$$\begin{aligned} \partial_t \mathbf{E} &= -D\nabla \times (\nabla \times \mathbf{E}) - 2\pi \mathbf{j} \\ &\quad - \hat{\mathbf{z}} \times \nabla \left(\frac{\lambda_+}{2} E^2 - \frac{\lambda_-}{2} \mathbf{E}^{\odot 2} + \eta \right). \end{aligned} \quad (35)$$

As a final step, as customary in “macroscopic” electrodynamics, we separate the contributions due to free and bound vortices by decomposing the vortex density and current as

$$\begin{aligned} n &= n_f + n_b, \\ \mathbf{j} &= \mathbf{j}_f + \mathbf{j}_b. \end{aligned} \quad (36)$$

Bound vortices lead to polarization of the medium, which can be described by a polarization density \mathbf{P} that satisfies

$$\begin{aligned} \nabla \cdot \mathbf{P} &= -2\pi n_b, \\ \partial_t \mathbf{P} &= 2\pi \mathbf{j}_b. \end{aligned} \quad (37)$$

Adding the polarization to the electric field we obtain the displacement field

$$\mathbf{D} = \mathbf{E} + 2\pi \mathbf{P} = (1 + 2\pi\chi) \mathbf{E} = \varepsilon \mathbf{E}, \quad (38)$$

where we set $\mathbf{P} = \chi \mathbf{E}$ with the susceptibility χ , and the last relation defines the dielectric constant $\varepsilon = 1 + 2\pi\chi$. We show below the even though we are considering an anisotropic system, to the lowest perturbative order in the KPZ non-linearity it is sufficient to consider a single isotropic dielectric constant instead of a dielectric tensor. With these definitions, Eqs. (30) and (35) can be written as

$$\nabla \cdot \mathbf{E} = \frac{2\pi}{\varepsilon} n_f, \quad (39)$$

and

$$\begin{aligned} \varepsilon \partial_t \mathbf{E} &= -D\nabla \times (\nabla \times \mathbf{E}) - 2\pi \mathbf{j}_f \\ &\quad - \hat{\mathbf{z}} \times \nabla \left(\frac{\lambda_+}{2} E^2 - \frac{\lambda_-}{2} \mathbf{E}^{\odot 2} + \eta \right). \end{aligned} \quad (40)$$

In the following, we drop the subscript f .

B. Perturbative calculation of the vortex interaction

As we are interested in the interaction of vortices, which is encoded in the deterministic dynamics, we set the noise to zero, $\eta = 0$. Moreover, we assume that the mobility of vortices is small. This allows us to consider the static limit [?] in which $\partial_t \mathbf{E} = \mathbf{j} = 0$. Then, Eq. (40) becomes

$$0 = D (\nabla^2 \mathbf{E} - 2\pi \nabla n) - \hat{\mathbf{z}} \times \nabla \left(\frac{\lambda_+}{2} E^2 - \frac{\lambda_-}{2} \mathbf{E}^{\odot 2} \right). \quad (41)$$

This equation and Eq. (39) determine the electrostatic field generated by a collection of free vortices with local density n . It is convenient to represent the electric field in terms of scalar and vector potentials,

$$\mathbf{E} = -\nabla \phi - \mathbf{A}. \quad (42)$$

As usual, this decomposition does not uniquely define the potentials. It is invariant under gauge transformations of the form $\phi' = \phi - \chi$ and $\mathbf{A}' = \mathbf{A} + \nabla \chi$. This redundancy can be eliminated by working in a particular gauge. Here, we impose the Lorenz gauge condition $\partial_t \phi + D\nabla \cdot \mathbf{A} = 0$, which in the static limit reduces to $\nabla \cdot \mathbf{A} = 0$. Then, the scalar potential encodes the longitudinal part of the electric field, and the vector potential the transverse part. It can be written in terms of another potential ψ as

$$\mathbf{A} = -\hat{\mathbf{z}} \times \nabla \psi. \quad (43)$$

Inserting Eqs. (42) and (43) in Eqs. (39) and (41), we obtain

$$-\nabla^2 \phi = \frac{2\pi}{\varepsilon} n, \quad (44)$$

$$D\nabla^2 \psi = \frac{\lambda_+}{2} (\nabla \phi - \hat{\mathbf{z}} \times \nabla \psi)^2 - \frac{\lambda_-}{2} (\nabla \phi - \hat{\mathbf{z}} \times \nabla \psi)^{\odot 2}. \quad (45)$$

These equations can be integrated with the aid of the fundamental solution of the Laplacian (i.e., the electrostatic potential generated by a point charge),

$$G(\mathbf{r}) = -\nabla^{-2} \delta(\mathbf{r}) = -\frac{1}{2\pi} \ln(r/a). \quad (46)$$

As usual, a is to be understood as a microscopic cutoff. Here and in the following, the potential $G(\mathbf{r})$ should be set to zero for $r < a$. With the aid of the fundamental solution (46), Eqs. (44) can be rewritten as convolution integrals,

$$\phi(\mathbf{r}) = \frac{2\pi}{\varepsilon} \int_{\mathbf{r}'} G(\mathbf{r} - \mathbf{r}') n(\mathbf{r}'), \quad (47)$$

and

$$\begin{aligned} \psi(\mathbf{r}) &= -\frac{1}{2D} \int_{\mathbf{r}'} G(\mathbf{r} - \mathbf{r}') \left[\lambda_+ (\nabla \phi(\mathbf{r}') - \hat{\mathbf{z}} \times \nabla \psi(\mathbf{r}'))^2 \right. \\ &\quad \left. - \lambda_- (\nabla \phi(\mathbf{r}') - \hat{\mathbf{z}} \times \nabla \psi(\mathbf{r}'))^{\odot 2} \right], \end{aligned} \quad (48)$$

where we write $\int_{\mathbf{r}} = \int d^2 \mathbf{r}$, and the integration extends over the area occupied by the system. While Eq. (47) fully determines the potential ϕ for a given charge distribution n , Eq. (48) is an integro-differential equation for ψ . By iterating this equation, we obtain a solution in the form of a perturbative expansion in λ_+ and λ_- ,

$$\psi = \frac{1}{\varepsilon} \psi^{(0)} + \frac{1}{\varepsilon^2} \psi^{(1)} + \frac{1}{\varepsilon^3} \psi^{(2)} + \dots \quad (49)$$

(we explicitly specify factors of $1/\varepsilon$ to get simpler expressions below). More concretely, setting $\lambda_+ = \lambda_- = 0$

in Eq. (48), we find that the zeroth-order contribution vanishes, $\psi^{(0)} = 0$. The first-order contribution $\psi^{(1)}$ can be obtained by inserting $\psi = \psi^{(0)} = 0$ on the RHS of Eq. (48). Another iteration yields the lowest-order terms,

$$\begin{aligned}\psi^{(1)} &= - \sum_{\sigma=\pm} \sigma \alpha_{\sigma} \psi_{\sigma}^{(1)}, \\ \psi^{(2)} &= - \sum_{\sigma=\pm} \alpha_{\sigma}^2 \psi_{\sigma}^{(2)} + \alpha_{+} \alpha_{-} \psi_{+-}^{(2)}.\end{aligned}\quad (50)$$

As in the previous section, we denote $\alpha_{\pm} = \lambda_{\pm}/(2D)$. The explicit expressions for the lowest-order terms read

$$\psi_{\sigma}^{(1)}(\mathbf{r}) = \varepsilon^2 \int_{\mathbf{r}'} G(\mathbf{r} - \mathbf{r}') (\nabla \phi(\mathbf{r}'))^{\odot 2}, \quad (51)$$

(here and in the following, for $\sigma = +$ the \odot product should be replaced by the usual scalar product)

$$\psi_{\sigma}^{(2)}(\mathbf{r}) = 2\varepsilon \int_{\mathbf{r}'} G(\mathbf{r} - \mathbf{r}') \left[\nabla \phi(\mathbf{r}') \odot \left(\hat{\mathbf{z}} \times \nabla \psi_{\sigma}^{(1)}(\mathbf{r}') \right) \right], \quad (52)$$

and the mixed term is given by

$$\begin{aligned}\psi_{+-}^{(2)}(\mathbf{r}) &= 2\varepsilon \int_{\mathbf{r}'} G(\mathbf{r} - \mathbf{r}') \left[\nabla \phi(\mathbf{r}') \cdot \left(\hat{\mathbf{z}} \times \nabla \psi_{-}^{(1)}(\mathbf{r}') \right) \right. \\ &\quad \left. + \nabla \phi(\mathbf{r}') \odot \left(\hat{\mathbf{z}} \times \nabla \psi_{+}^{(1)}(\mathbf{r}') \right) \right].\end{aligned}\quad (53)$$

The above expressions are valid for any charge distribution n . In the following, we consider a dipole which is described by

$$n(\mathbf{r}) = \delta(\mathbf{r} - \mathbf{r}_{+}) - \delta(\mathbf{r} - \mathbf{r}_{-}). \quad (54)$$

Inserting this in Eq. (47) yields the scalar electrostatic potential generated by the dipole:

$$\phi(\mathbf{r}) = \frac{2\pi}{\varepsilon} (G(\mathbf{r} - \mathbf{r}_{+}) - G(\mathbf{r} - \mathbf{r}_{-})) = \frac{1}{\varepsilon} \ln \left| \frac{\mathbf{r} - \mathbf{r}_{+}}{\mathbf{r} - \mathbf{r}_{-}} \right|. \quad (55)$$

Equations (51), (52), and (53) require the gradient of the scalar potential. In terms of

$$\mathbf{f}(\mathbf{r}) = 2\pi \nabla G(\mathbf{r}) = -\frac{\mathbf{r}}{r^2}, \quad (56)$$

we find

$$\begin{aligned}\nabla \phi(\mathbf{r}) &= \frac{1}{\varepsilon} (\mathbf{f}(\mathbf{r} - \mathbf{r}_{+}) - \mathbf{f}(\mathbf{r} - \mathbf{r}_{-})) \\ &= -\frac{1}{\varepsilon} \left(\frac{\mathbf{r} - \mathbf{r}_{+}}{|\mathbf{r} - \mathbf{r}_{+}|^2} - \frac{\mathbf{r} - \mathbf{r}_{-}}{|\mathbf{r} - \mathbf{r}_{-}|^2} \right).\end{aligned}\quad (57)$$

Inserting this in Eqs. (51) and (52) yields

$$\psi_{\sigma}^{(1)}(\mathbf{r}) = \int_{\mathbf{r}'} G(\mathbf{r} - \mathbf{r}') (\mathbf{f}(\mathbf{r}' - \mathbf{r}_{+}) - \mathbf{f}(\mathbf{r}' - \mathbf{r}_{-}))^{\odot 2}, \quad (58)$$

and

$$\begin{aligned}\psi_{\sigma}^{(2)}(\mathbf{r}) &= 2 \int_{\mathbf{r}'} G(\mathbf{r} - \mathbf{r}') \left[(\mathbf{f}(\mathbf{r}' - \mathbf{r}_{+}) - \mathbf{f}(\mathbf{r}' - \mathbf{r}_{-})) \right. \\ &\quad \left. \odot \left(\hat{\mathbf{z}} \times \nabla \psi_{\sigma}^{(1)}(\mathbf{r}') \right) \right],\end{aligned}\quad (59)$$

and from Eq. (53) we obtain

$$\begin{aligned}\psi_{+-}^{(2)}(\mathbf{r}) &= 2 \int_{\mathbf{r}'} G(\mathbf{r} - \mathbf{r}') (\mathbf{f}(\mathbf{r}' - \mathbf{r}_{+}) - \mathbf{f}(\mathbf{r}' - \mathbf{r}_{-}))^T \\ &\quad \left[\left(\hat{\mathbf{z}} \times \nabla \psi_{-}^{(1)}(\mathbf{r}') \right) + \sigma_z \left(\hat{\mathbf{z}} \times \nabla \psi_{+}^{(1)}(\mathbf{r}') \right) \right],\end{aligned}\quad (60)$$

where we used that with the Pauli matrix σ_z the \odot product can be written as $\mathbf{a} \odot \mathbf{b} = a_x b_x - a_y b_y = \mathbf{a}^T \sigma_z \mathbf{b}$.

The integrals in the above expressions for the lowest-order contributions to ψ are divergent in the thermodynamic limit. This complication is resolved upon taking the gradient as required by Eq. (43). Therefore, in the following we find it convenient to consider $\mathbf{a} = \nabla \psi$. In analogy to Eqs. (49) and (50) we write

$$\mathbf{a} = \frac{1}{\varepsilon^2} \mathbf{a}^{(1)} + \frac{1}{\varepsilon^3} \mathbf{a}^{(2)} + \dots, \quad (61)$$

(recall that $\psi^{(0)} = 0$) and

$$\begin{aligned}\mathbf{a}^{(1)} &= - \sum_{\sigma=\pm} \sigma \alpha_{\sigma} \mathbf{a}_{\sigma}^{(1)}, \\ \mathbf{a}^{(2)} &= - \sum_{\sigma=\pm} \alpha_{\sigma}^2 \mathbf{a}_{\sigma}^{(2)} + \alpha_{+} \alpha_{-} \mathbf{a}_{+-}^{(2)},\end{aligned}\quad (62)$$

where

$$\mathbf{a}_{\sigma}^{(1)}(\mathbf{r}) = \frac{1}{2\pi} \int_{\mathbf{r}'} \mathbf{f}(\mathbf{r} - \mathbf{r}') (\mathbf{f}(\mathbf{r}' - \mathbf{r}_{+}) - \mathbf{f}(\mathbf{r}' - \mathbf{r}_{-}))^{\odot 2}, \quad (63)$$

and

$$\begin{aligned}\mathbf{a}_{\sigma}^{(2)}(\mathbf{r}) &= \frac{1}{\pi} \int_{\mathbf{r}'} \mathbf{f}(\mathbf{r} - \mathbf{r}') \left[(\mathbf{f}(\mathbf{r}' - \mathbf{r}_{+}) - \mathbf{f}(\mathbf{r}' - \mathbf{r}_{-})) \right. \\ &\quad \left. \odot \left(\hat{\mathbf{z}} \times \mathbf{a}_{\sigma}^{(1)}(\mathbf{r}') \right) \right],\end{aligned}\quad (64)$$

and finally

$$\begin{aligned}\mathbf{a}_{+-}^{(2)}(\mathbf{r}) &= \frac{1}{\pi} \int_{\mathbf{r}'} \mathbf{f}(\mathbf{r} - \mathbf{r}') (\mathbf{f}(\mathbf{r}' - \mathbf{r}_{+}) - \mathbf{f}(\mathbf{r}' - \mathbf{r}_{-}))^T \\ &\quad \left[\left(\hat{\mathbf{z}} \times \mathbf{a}_{-}^{(1)}(\mathbf{r}') \right) + \sigma_z \left(\hat{\mathbf{z}} \times \mathbf{a}_{+}^{(1)}(\mathbf{r}') \right) \right].\end{aligned}\quad (65)$$

In terms of the quantities defined above, the vector potential is given by $\mathbf{A} = -\hat{\mathbf{z}} \times \mathbf{a}$, and up to second order in the KPZ non-linearity the static electric field can be written as

$$\mathbf{E} = \frac{1}{\varepsilon} \mathbf{E}^{(0)} - \sum_{\sigma=\pm} \left[\frac{\sigma \alpha_{\sigma}}{\varepsilon^2} \mathbf{E}_{\sigma}^{(1)} + \frac{\alpha_{\sigma}^2}{\varepsilon^3} \mathbf{E}_{\sigma}^{(2)} \right] + \frac{\alpha_{+} \alpha_{-}}{\varepsilon^3} \mathbf{E}_{+-}^{(2)}, \quad (66)$$

where

$$\begin{aligned}\mathbf{E}^{(0)}(\mathbf{r}) &= -\varepsilon \nabla \phi(\mathbf{r}), \\ \mathbf{E}_{\sigma}^{(1,2)}(\mathbf{r}) &= \hat{\mathbf{z}} \times \mathbf{a}_{\sigma}^{(1,2)}(\mathbf{r}), \\ \mathbf{E}_{+-}^{(2)}(\mathbf{r}) &= \hat{\mathbf{z}} \times \mathbf{a}_{+-}^{(2)}(\mathbf{r}).\end{aligned}\quad (67)$$

In the following sections, we evaluate the integrals in Eqs. (63), (64), and (65) both analytically and — to check the rather lengthy analytical calculations — numerically. For completeness, we also repeat the calculation of the purely isotropic corrections, which can also be found in Ref. [?]. Actually, we do not need to find the electric field at arbitrary points in space, since the force acting on the charges is determined by the electric field at the position of one of the charges. Therefore, we evaluate the second-order corrections (64) and (65) only at $\mathbf{r} = \mathbf{r}_+$. The first-order correction (63), however, has to be calculated for any \mathbf{r} , since it is required in (64) and (65).

Equations (63), (64), and (65) are integrals over products of the function $\mathbf{f}(\mathbf{r})$ defined in Eq. (56) with different arguments. The pole of $\mathbf{f}(\mathbf{r}) = -\mathbf{r}/r^2$ at $\mathbf{r} = 0$, which is cut off at the scale a , can lead to logarithmic contributions to the integrals in the limit $a \rightarrow 0$. In some cases, these singular contributions are lifted by the angular integration. The main theme of the calculation we present in the following is therefore to identify the poles that do give singular contributions. Once these poles have been identified, the integrals can be evaluated by shifting the integration variable such that the “dangerous” poles are at the origin $\mathbf{r} = 0$, and the corresponding integration has to be cut at $r = a$, while the remaining integrals can be extended over the entire plane.

1. First order correction

We split the first order correction in Eq. (63) into three contributions

$$\mathbf{a}_\sigma^{(1)}(\mathbf{r}) = \mathbf{a}_{\sigma,+}^{(1)}(\mathbf{r}) - 2\mathbf{a}_{\sigma,+}^{(1)}(\mathbf{r}) + \mathbf{a}_{\sigma,-}^{(1)}(\mathbf{r}), \quad (68)$$

where (recall that for $\sigma = +$ the \odot product should be replaced by the usual scalar product)

$$\mathbf{a}_{\sigma,\pm}^{(1)}(\mathbf{r}) = \frac{1}{2\pi} \int_{\mathbf{r}'} \mathbf{f}(\mathbf{r} - \mathbf{r}') \mathbf{f}(\mathbf{r}' - \mathbf{r}_\pm) \odot^2, \quad (69)$$

$$\mathbf{a}_{\sigma,+}^{(1)}(\mathbf{r}) = \frac{1}{2\pi} \int_{\mathbf{r}'} \mathbf{f}(\mathbf{r} - \mathbf{r}') (\mathbf{f}(\mathbf{r}' - \mathbf{r}_+) \odot \mathbf{f}(\mathbf{r}' - \mathbf{r}_-)). \quad (70)$$

Let's consider $\mathbf{a}_{\sigma,\pm}^{(1)}(\mathbf{r})$ first. Shifting the integration variable as $\mathbf{r}' \rightarrow \mathbf{r}' + \mathbf{r}_\pm$ and denoting $\mathbf{R}_\pm = \mathbf{r} - \mathbf{r}_\pm$, we obtain

$$\mathbf{a}_{\sigma,\pm}^{(1)}(\mathbf{r}) = \frac{1}{2\pi} \int_{\mathbf{r}'} \mathbf{f}(\mathbf{R}_\pm - \mathbf{r}') \mathbf{f}(\mathbf{r}') \odot^2. \quad (71)$$

This and many of the following integrals are conveniently performed using MATHEMATICA, resulting in

$$\mathbf{a}_{+,\pm}^{(1)}(\mathbf{r}) = \mathbf{f}(\mathbf{R}_\pm) \ln(R_\pm/a), \quad (72)$$

$$\mathbf{a}_{-,\pm}^{(1)}(\mathbf{r}) = \mathbf{e}(\mathbf{R}_\pm), \quad (73)$$

where

$$\begin{aligned} \mathbf{e}(\mathbf{r}) &= -\frac{\cos(\theta) \sin(\theta)}{r} \begin{pmatrix} -\sin(\theta) \\ \cos(\theta) \end{pmatrix} \\ &= -\cos(\theta) \sin(\theta) \frac{\hat{\mathbf{z}} \times \mathbf{r}}{r^2} = -xy \frac{\hat{\mathbf{z}} \times \mathbf{r}}{r^4}. \end{aligned} \quad (74)$$

Note that these expressions are valid for $R_\pm > a$ and should be set to zero below the cutoff a .

The calculation of $\mathbf{a}_{\sigma,+}^{(1)}(\mathbf{r})$ is more involved. In Eq. (70), we replace $\mathbf{r}' \rightarrow \mathbf{r}' + \mathbf{r}$ and as above we write $\mathbf{R}_\pm = \mathbf{r} - \mathbf{r}_\pm$, which yields

$$\begin{aligned} \mathbf{a}_{\sigma,+}^{(1)}(\mathbf{r}) &= -\frac{1}{2\pi} \int_{\mathbf{r}'} \mathbf{f}(\mathbf{r}') (\mathbf{f}(\mathbf{r}' + \mathbf{R}_+) \odot \mathbf{f}(\mathbf{r}' + \mathbf{R}_-)) \\ &= \frac{1}{2\pi} \int_{\mathbf{r}'} \frac{\mathbf{r}'}{r'^2} \frac{(\mathbf{r}' + \mathbf{R}_+) \odot (\mathbf{r}' + \mathbf{R}_-)}{|\mathbf{r}' + \mathbf{R}_+|^2 |\mathbf{r}' + \mathbf{R}_-|^2}. \end{aligned} \quad (75)$$

To evaluate these integrals, we switch to polar coordinates for \mathbf{r}' and \mathbf{R}_\pm :

$$\mathbf{r}' = r' \begin{pmatrix} \cos(\theta' + \theta_+) \\ \sin(\theta' + \theta_+) \end{pmatrix}, \quad \mathbf{R}_\pm = R_\pm \begin{pmatrix} \cos(\theta_\pm) \\ \sin(\theta_\pm) \end{pmatrix}. \quad (76)$$

Moreover, we use the following Fourier-cosine series:

$$\begin{aligned} \frac{1}{|\mathbf{r}' + \mathbf{R}_-|^2} &= \frac{1}{|r'^2 - R_-^2|} \sum_{n=0}^{\infty} (2 - \delta_{n,0}) \\ &\quad \times \left(-\frac{r_{<}}{r_{>}} \right)^n \cos(n(\theta' + \theta_+ - \theta_-)), \end{aligned} \quad (77)$$

where $r_{<}$ and $r_{>}$ are the lesser and greater, respectively, of r' and R_- . Finally, we set

$$\frac{1}{|\mathbf{r}' + \mathbf{R}_+|^2} = \frac{1}{r'^2 + R_+^2} \frac{1}{1 + s' \cos(\theta')}, \quad s' = \frac{2r'R_+}{r'^2 + R_+^2}. \quad (78)$$

Then, Eq. (70) becomes

$$\begin{aligned} \mathbf{a}_{\sigma,+}^{(1)}(\mathbf{r}) &= \frac{1}{2\pi} \sum_{n=0}^{\infty} (2 - \delta_{n,0}) \int_{\mathbf{r}'} \frac{1}{r'^2} \frac{1}{r'^2 + R_+^2} \\ &\quad \times \frac{1}{|r'^2 - R_-^2|} \left(-\frac{r_{<}}{r_{>}} \right)^n \cos(n(\theta' + \theta_+ - \theta_-)) \\ &\quad \times \mathbf{r}' \frac{(\mathbf{r}' + \mathbf{R}_+) \odot (\mathbf{r}' + \mathbf{R}_-)}{1 + s' \cos(\theta')}. \end{aligned} \quad (79)$$

After some lengthy but straightforward algebra, the angular integrals can be performed using the relation [?]

$$\int_0^{2\pi} d\theta \frac{\cos(n\theta)}{1 + s \cos(\theta)} = \frac{2\pi}{\sqrt{1 - s^2}} \left(\frac{\sqrt{1 - s^2} - 1}{s} \right)^n, \quad (80)$$

which holds for $s^2 < 1$ and $n \geq 0$. In the resulting expression, the summation over n can be carried out, and finally performing the integral over r' yields the result:

$$\mathbf{a}_{+,\pm}^{(1)}(\mathbf{r}) = -\frac{1}{2} (\mathbf{f}(\mathbf{R}_+) \ln(R/R_-) + \mathbf{f}(\mathbf{R}_-) \ln(R/R_+)), \quad (81)$$

where R is the magnitude of $\mathbf{R} = \mathbf{r}_+ - \mathbf{r}_-$. We omit the cumbersome expression for $\mathbf{a}_{\sigma,+}^{(1)}(\mathbf{r})$. Combining these results with Eqs. (72) and (73) gives the first order correction $\mathbf{E}^{(1)}(\mathbf{r})$. Again, we omit the rather lengthy expression.

The calculation of $\mathbf{a}_{\sigma,+}^{(1)}(\mathbf{r})$ is actually much simpler for the special case $\mathbf{r} = \mathbf{r}_+$ that gives the electric field acting on the charge at \mathbf{r}_+ . Then, shifting $\mathbf{r}' \rightarrow \mathbf{r} + \mathbf{r}_+$, Eq. (70) becomes

$$\mathbf{a}_{\sigma,+}^{(1)}(\mathbf{r}_+) = -\frac{1}{2\pi} \int_{\mathbf{r}} \mathbf{f}(\mathbf{r}) (\mathbf{f}(\mathbf{r}) \odot \mathbf{f}(\mathbf{r} + \mathbf{R})), \quad (82)$$

where we used $\mathbf{f}(-\mathbf{r}) = -\mathbf{f}(\mathbf{r})$. Again, MATHEMATICA does the job, and combining the result with Eqs. (72)

and (73) we obtain

$$\mathbf{a}_+^{(1)}(\mathbf{r}_+) = \frac{1}{2} \mathbf{f}(\mathbf{R}) (4 \ln(R/a) - 1), \quad (83)$$

$$\mathbf{a}_-^{(1)}(\mathbf{r}_+) = \frac{3}{2} \mathbf{f}(\mathbf{R}) \cos(2\theta_{\mathbf{R}}) - \frac{1}{R^2} \begin{pmatrix} R_x \\ -R_y \end{pmatrix} (\ln(R/a) - 1), \quad (84)$$

where we used the polar representation of \mathbf{R} ,

$$\mathbf{R} = \begin{pmatrix} R_x \\ R_y \end{pmatrix} = R \begin{pmatrix} \cos(\theta_{\mathbf{R}}) \\ \sin(\theta_{\mathbf{R}}) \end{pmatrix}. \quad (85)$$

Equations (83) and (84) give the first order corrections to the electric field at the position of the positive charge,

$$\mathbf{E}_+^{(1)}(\mathbf{r}_+) = \frac{1}{2} \hat{\mathbf{z}} \times \mathbf{f}(\mathbf{R}) (4 \ln(R/a) - 1), \quad (86)$$

and

$$\mathbf{E}_-^{(1)}(\mathbf{r}_+) = \frac{3}{2} \hat{\mathbf{z}} \times \mathbf{f}(\mathbf{R}) \cos(2\theta_{\mathbf{R}}) - \frac{1}{R^2} \begin{pmatrix} R_y \\ R_x \end{pmatrix} (\ln(R/a) - 1). \quad (87)$$

2. Second order correction: diagonal terms

For $\mathbf{r} = \mathbf{r}_+$, the second-order correction Eq. (64) becomes

$$\mathbf{a}_{\sigma}^{(2)}(\mathbf{r}_+) = -\frac{1}{\pi} \int_{\mathbf{r}} \mathbf{f}(\mathbf{r}) \left[(\mathbf{f}(\mathbf{r}) - \mathbf{f}(\mathbf{r} + \mathbf{R})) \odot \left(\hat{\mathbf{z}} \times \mathbf{a}_{\sigma}^{(1)}(\mathbf{r} + \mathbf{r}_+) \right) \right]. \quad (88)$$

We decompose the second order correction in two contributions,

$$\mathbf{a}_{\sigma}^{(2)}(\mathbf{r}_+) = \mathbf{a}_{\sigma,1}^{(2)}(\mathbf{r}_+) + \mathbf{a}_{\sigma,2}^{(2)}(\mathbf{r}_+), \quad (89)$$

where (cf. Eq. (68))

$$\begin{aligned} \mathbf{a}_{\sigma,1}^{(2)}(\mathbf{r}_+) &= -\frac{1}{\pi} \int_{\mathbf{r}} \mathbf{f}(\mathbf{r}) \left\{ (\mathbf{f}(\mathbf{r}) - \mathbf{f}(\mathbf{r} + \mathbf{R})) \odot \left[\hat{\mathbf{z}} \times \left(\mathbf{a}_{\sigma,+}^{(1)}(\mathbf{r} + \mathbf{r}_+) + \mathbf{a}_{\sigma,-}^{(1)}(\mathbf{r} + \mathbf{r}_+) \right) \right] \right\}, \\ \mathbf{a}_{\sigma,2}^{(2)}(\mathbf{r}_+) &= \frac{2}{\pi} \int_{\mathbf{r}} \mathbf{f}(\mathbf{r}) \left[(\mathbf{f}(\mathbf{r}) - \mathbf{f}(\mathbf{r} + \mathbf{R})) \odot \left(\hat{\mathbf{z}} \times \mathbf{a}_{\sigma,+}^{(1)}(\mathbf{r} + \mathbf{r}_+) \right) \right]. \end{aligned} \quad (90)$$

To proceed with the calculation of $\mathbf{a}_{\sigma,1}^{(2)}(\mathbf{r}_+)$, we have to specify whether we are dealing with the isotropic or fully anisotropic case. Before going into that, let us simplify the expression for $\mathbf{a}_{\sigma,2}^{(2)}(\mathbf{r}_+)$. Here, ‘‘simplifying’’ refers to splitting into two parts,

$$\mathbf{a}_{\sigma,2}^{(2)}(\mathbf{r}_+) = \mathbf{a}_{\sigma,2,1}^{(2)}(\mathbf{r}_+) + \mathbf{a}_{\sigma,2,2}^{(2)}(\mathbf{r}_+), \quad (91)$$

where

$$\mathbf{a}_{\sigma,2,1}^{(2)}(\mathbf{r}_+) = \frac{2}{\pi} \int_{\mathbf{r}} \mathbf{f}(\mathbf{r}) \left[\mathbf{f}(\mathbf{r}) \odot \left(\hat{\mathbf{z}} \times \mathbf{a}_{\sigma,+}^{(1)}(\mathbf{r} + \mathbf{r}_+) \right) \right], \quad (92)$$

$$\mathbf{a}_{\sigma,2,2}^{(2)}(\mathbf{r}_+) = -\frac{2}{\pi} \int_{\mathbf{r}} \mathbf{f}(\mathbf{r}) \left[\mathbf{f}(\mathbf{r} + \mathbf{R}) \odot \left(\hat{\mathbf{z}} \times \mathbf{a}_{\sigma,+}^{(1)}(\mathbf{r} + \mathbf{r}_+) \right) \right]. \quad (93)$$

Copying from Eq. (70), we find

$$\mathbf{a}_{\sigma,+}^{(1)}(\mathbf{r} + \mathbf{r}_+) = \frac{1}{2\pi} \int_{\mathbf{r}'} \mathbf{f}(\mathbf{r} + \mathbf{r}_+ - \mathbf{r}') (\mathbf{f}(\mathbf{r}' - \mathbf{r}_+) \odot \mathbf{f}(\mathbf{r}' - \mathbf{r}_-)) = \frac{1}{2\pi} \int_{\mathbf{r}'} \mathbf{f}(\mathbf{r} - \mathbf{r}') (\mathbf{f}(\mathbf{r}') \odot \mathbf{f}(\mathbf{r}' + \mathbf{R})). \quad (94)$$

Then, we can write Eq. (92) as

$$\mathbf{a}_{\sigma,2,1}^{(2)}(\mathbf{r}_+) = \frac{1}{\pi^2} \int_{\mathbf{r},\mathbf{r}'} \mathbf{f}(\mathbf{r}) [\mathbf{f}(\mathbf{r}) \odot (\hat{\mathbf{z}} \times \mathbf{f}(\mathbf{r} - \mathbf{r}'))] (\mathbf{f}(\mathbf{r}') \odot \mathbf{f}(\mathbf{r}' + \mathbf{R})) = \frac{2}{\pi} \int_{\mathbf{r}'} \mathbf{c}_\sigma(\mathbf{r}') (\mathbf{f}(\mathbf{r}') \odot \mathbf{f}(\mathbf{r}' + \mathbf{R})), \quad (95)$$

where

$$\mathbf{c}_\sigma(\mathbf{r}') = \frac{1}{2\pi} \int_{\mathbf{r}} \mathbf{f}(\mathbf{r}) [\mathbf{f}(\mathbf{r}) \odot (\hat{\mathbf{z}} \times \mathbf{f}(\mathbf{r} - \mathbf{r}'))]. \quad (96)$$

Finally, plugging Eq. (94) into Eq. (93), the latter becomes

$$\mathbf{a}_{\sigma,2,2}^{(2)}(\mathbf{r}_+) = -\frac{1}{\pi^2} \int_{\mathbf{r},\mathbf{r}'} \mathbf{f}(\mathbf{r}) [\mathbf{f}(\mathbf{r} + \mathbf{R}) \odot (\hat{\mathbf{z}} \times \mathbf{f}(\mathbf{r} - \mathbf{r}'))] (\mathbf{f}(\mathbf{r}') \odot \mathbf{f}(\mathbf{r}' + \mathbf{R})). \quad (97)$$

So far, we have split the second order correction into three contributions, given by Eqs. (90), (95), and (97). In the following, we calculate those, first for $\sigma = +$ and then for $\sigma = -$.

a. $\sigma = +$ We start with $\mathbf{a}_{+,1}^{(2)}(\mathbf{r}_+)$ defined in Eq. (90). Using Eq. (72) we obtain

$$\mathbf{a}_{+,+}^{(1)}(\mathbf{r} + \mathbf{r}_+) + \mathbf{a}_{+,-}^{(1)}(\mathbf{r} + \mathbf{r}_+) = \mathbf{f}(\mathbf{r}) \ln(r/a) + \mathbf{f}(\mathbf{r} + \mathbf{R}) \ln(|\mathbf{r} + \mathbf{R}|/a), \quad (98)$$

and inserting this relation in Eq. (90) leaves us with

$$\begin{aligned} \mathbf{a}_{+,1}^{(2)}(\mathbf{r}_+) &= \frac{1}{\pi} \int_{\mathbf{r}} \mathbf{f}(\mathbf{r}) \{ \hat{\mathbf{z}} \cdot [(\mathbf{f}(\mathbf{r}) - \mathbf{f}(\mathbf{r} + \mathbf{R})) \times (\mathbf{f}(\mathbf{r}) \ln(r/a) + \mathbf{f}(\mathbf{r} + \mathbf{R}) \ln(|\mathbf{r} + \mathbf{R}|/a))] \} \\ &= \frac{1}{\pi} \int_{\mathbf{r}} \mathbf{f}(\mathbf{r}) [\hat{\mathbf{z}} \cdot (\mathbf{f}(\mathbf{r}) \times \mathbf{f}(\mathbf{r} + \mathbf{R}))] \ln(r|\mathbf{r} + \mathbf{R}|/a^2) \\ &= \mathbf{b}_1(\mathbf{R}) + \mathbf{b}_2(\mathbf{R}), \end{aligned} \quad (99)$$

where

$$\mathbf{b}_1(\mathbf{R}) = \frac{1}{\pi} \int_{\mathbf{r}} \mathbf{f}(\mathbf{r}) [\hat{\mathbf{z}} \cdot (\mathbf{f}(\mathbf{r}) \times \mathbf{f}(\mathbf{r} + \mathbf{R}))] \ln(rR/a^2), \quad (100)$$

$$\mathbf{b}_2(\mathbf{R}) = \frac{1}{\pi} \int_{\mathbf{r}} \mathbf{f}(\mathbf{r}) [\hat{\mathbf{z}} \cdot (\mathbf{f}(\mathbf{r}) \times \mathbf{f}(\mathbf{r} + \mathbf{R}))] \ln(|\mathbf{r} + \mathbf{R}|/R) = \frac{1}{\pi} \int_{\mathbf{r}} \mathbf{f}(\mathbf{r} - \mathbf{R}) [\hat{\mathbf{z}} \cdot (\mathbf{f}(\mathbf{r} - \mathbf{R}) \times \mathbf{f}(\mathbf{r}))] \ln(r/R). \quad (101)$$

The results read as follows:

$$\mathbf{b}_1(\mathbf{R}) = -\frac{1}{4} \hat{\mathbf{z}} \times \mathbf{f}(\mathbf{R}) (6 \ln(R/a)^2 + 4 \ln(R/a) + 1), \quad (102)$$

$$\mathbf{b}_2(\mathbf{R}) = 0, \quad (103)$$

and hence we obtain for the first part of the second order correction:

$$\mathbf{a}_{+,1}^{(2)}(\mathbf{r}_+) = \mathbf{b}_1(\mathbf{R}). \quad (104)$$

We move on to calculate $\mathbf{a}_{+,2,1}^{(2)}(\mathbf{r}_+)$, given by Eq. (95), and find

$$\mathbf{a}_{+,2,1}^{(2)}(\mathbf{r}_+) = -\frac{1}{2} \hat{\mathbf{z}} \times \mathbf{f}(\mathbf{R}) (\ln(R/a)^2 - 1). \quad (105)$$

The nastiest part by far is $\mathbf{a}_{+,2,2}^{(2)}(\mathbf{r}_+)$, which can be written as

$$\begin{aligned} \mathbf{a}_{+,2,2}^{(2)}(\mathbf{r}_+) &= -\frac{1}{\pi^2} \int_{\mathbf{r},\mathbf{r}'} \mathbf{f}(\mathbf{r}) [\mathbf{f}(\mathbf{r} + \mathbf{R}) \cdot (\hat{\mathbf{z}} \times \mathbf{f}(\mathbf{r} - \mathbf{r}'))] (\mathbf{f}(\mathbf{r}') \cdot \mathbf{f}(\mathbf{r}' + \mathbf{R})) \\ &= -\frac{1}{\pi^2} \int_{\mathbf{r},\mathbf{r}'} \mathbf{f}(\mathbf{r}) [\hat{\mathbf{z}} \cdot (\mathbf{f}(\mathbf{r} - \mathbf{r}') \times \mathbf{f}(\mathbf{r} + \mathbf{R}))] (\mathbf{f}(\mathbf{r}') \cdot \mathbf{f}(\mathbf{r}' + \mathbf{R})) \\ &= \frac{1}{\pi^2} \int_{\mathbf{r},\mathbf{r}'} \frac{\mathbf{r} \cdot \hat{\mathbf{z}} \cdot [\mathbf{r} \times \mathbf{R} - \mathbf{r}' \times (\mathbf{r} + \mathbf{R})]}{r^2 |\mathbf{r} - \mathbf{r}'|^2 |\mathbf{r} + \mathbf{R}|^2} \frac{\mathbf{r}' \cdot (\mathbf{r}' + \mathbf{R})}{r'^2 |\mathbf{r}' + \mathbf{R}|^2}. \end{aligned} \quad (106)$$

To evaluate these integrals, we switch to polar coordinates for \mathbf{r} , \mathbf{r}' , and \mathbf{R} :

$$\mathbf{r} = r \begin{pmatrix} \cos(\theta + \theta_{\mathbf{R}}) \\ \sin(\theta + \theta_{\mathbf{R}}) \end{pmatrix}, \quad \mathbf{r}' = r' \begin{pmatrix} \cos(\theta' + \theta_{\mathbf{R}}) \\ \sin(\theta' + \theta_{\mathbf{R}}) \end{pmatrix}, \quad \mathbf{R} = R \begin{pmatrix} \cos(\theta_{\mathbf{R}}) \\ \sin(\theta_{\mathbf{R}}) \end{pmatrix}. \quad (107)$$

Moreover, we use the following Fourier-cosine series:

$$\frac{1}{|\mathbf{r} - \mathbf{r}'|^2} = \frac{1}{|r^2 - r'^2|} \sum_{n=0}^{\infty} (2 - \delta_{n,0}) \left(\frac{r_{<}}{r_{>}} \right)^n \cos(n(\theta - \theta')), \quad (108)$$

where $r_{<}$ and $r_{>}$ are the lesser and greater, respectively, of r and r' . Finally, we write

$$\frac{1}{|\mathbf{r} + \mathbf{R}|^2} = \frac{1}{r^2 + R^2} \frac{1}{1 + s \cos(\theta)}, \quad s = \frac{2rR}{r^2 + R^2}, \quad (109)$$

and we use an analogous representation with \mathbf{r} replaced by \mathbf{r}' . This leads us to

$$\begin{aligned} \mathbf{a}_{+,2,2}^{(2)}(\mathbf{r}_+) &= \frac{1}{\pi^2} \sum_{n=0}^{\infty} (2 - \delta_{n,0}) \int_{\mathbf{r}, \mathbf{r}'} \frac{1}{r^2 + R^2} \frac{1}{r'^2 + R^2} \frac{1}{|r^2 - r'^2|} \left(\frac{r_{<}}{r_{>}} \right)^n \cos(n(\theta - \theta')) \\ &\quad \times \frac{\mathbf{r}}{r^2 r'^2} \frac{\hat{\mathbf{z}} \cdot [\mathbf{r} \times \mathbf{R} - \mathbf{r}' \times (\mathbf{r} + \mathbf{R})]}{1 + s \cos(\theta)} \frac{\mathbf{r}' \cdot (\mathbf{r}' + \mathbf{R})}{1 + s' \cos(\theta')}. \end{aligned} \quad (110)$$

We then proceed to symmetrize the integrand with respect to $\theta \rightarrow -\theta$ and $\theta' \rightarrow -\theta'$, and to rearrange the trigonometric functions in the numerator such that the angular integrals can be preformed using Eq. (80). In the result, the summation over n can be carried out straightforwardly. Performing the integrals over r and r' leads us to

$$\mathbf{a}_{+,2,2}^{(2)}(\mathbf{r}_+) = 0. \quad (111)$$

Hence, the second order correction to the electric field at the position of the positive charge is given by

$$\mathbf{E}_+^{(2)}(\mathbf{r}_+) = \hat{\mathbf{z}} \times \mathbf{a}_{+,1}^{(2)}(\mathbf{r}_+) + \hat{\mathbf{z}} \times \mathbf{a}_{+,2,1}^{(2)}(\mathbf{r}_+) = \frac{1}{4} \mathbf{f}(\mathbf{R}) (8 \ln(R/a)^2 + 4 \ln(R/a) - 1). \quad (112)$$

b. $\sigma = -$ According to Eq. (73),

$$\begin{aligned} \hat{\mathbf{z}} \times \left(\mathbf{a}_{-,+}^{(1)}(\mathbf{r} + \mathbf{r}_+) + \mathbf{a}_{-,-}^{(1)}(\mathbf{r} + \mathbf{r}_+) \right) &= \hat{\mathbf{z}} \times (\mathbf{e}(\mathbf{r}) + \mathbf{e}(\mathbf{r} + \mathbf{R})) \\ &= -\cos(\theta) \sin(\theta) \mathbf{f}(\mathbf{r}) - \cos(\theta_{\mathbf{r}+\mathbf{R}}) \sin(\theta_{\mathbf{r}+\mathbf{R}}) \mathbf{f}(\mathbf{r} + \mathbf{R}), \end{aligned} \quad (113)$$

where we used

$$\hat{\mathbf{z}} \times \mathbf{e}(\mathbf{r}) = \cos(\theta) \sin(\theta) \frac{\mathbf{r}}{r^2} = -\cos(\theta) \sin(\theta) \mathbf{f}(\mathbf{r}). \quad (114)$$

Inserting Eq. (113) in Eq. (90), we obtain

$$\begin{aligned} \mathbf{a}_{-,1}^{(2)}(\mathbf{r}_+) &= \frac{1}{\pi} \int_{\mathbf{r}} \mathbf{f}(\mathbf{r}) [(\mathbf{f}(\mathbf{r}) - \mathbf{f}(\mathbf{r} + \mathbf{R})) \odot (\cos(\theta) \sin(\theta) \mathbf{f}(\mathbf{r}) + \cos(\theta_{\mathbf{r}+\mathbf{R}}) \sin(\theta_{\mathbf{r}+\mathbf{R}}) \mathbf{f}(\mathbf{r} + \mathbf{R}))] \\ &= \mathbf{k}_1(\mathbf{R}) + \mathbf{k}_2(\mathbf{R}) + \mathbf{k}_3(\mathbf{R}), \end{aligned} \quad (115)$$

where

$$\mathbf{k}_1(\mathbf{R}) = \frac{1}{\pi} \int_{\mathbf{r}} \cos(\theta) \sin(\theta) \mathbf{f}(\mathbf{r}) [(\mathbf{f}(\mathbf{r}) - \mathbf{f}(\mathbf{r} + \mathbf{R})) \odot \mathbf{f}(\mathbf{r})], \quad (116)$$

$$\mathbf{k}_2(\mathbf{R}) = -\frac{1}{\pi} \int_{\mathbf{r}} \cos(\theta_{\mathbf{r}+\mathbf{R}}) \sin(\theta_{\mathbf{r}+\mathbf{R}}) \mathbf{f}(\mathbf{r}) (\mathbf{f}(\mathbf{r} + \mathbf{R}))^{\odot 2} \quad (117)$$

$$= -\frac{1}{\pi} \int_{\mathbf{r}} \cos(\theta) \sin(\theta) \mathbf{f}(\mathbf{r} - \mathbf{R}) (\mathbf{f}(\mathbf{r}))^{\odot 2}, \quad (118)$$

$$\mathbf{k}_3(\mathbf{R}) = \frac{1}{\pi} \int_{\mathbf{r}} \cos(\theta_{\mathbf{r}+\mathbf{R}}) \sin(\theta_{\mathbf{r}+\mathbf{R}}) \mathbf{f}(\mathbf{r}) (\mathbf{f}(\mathbf{r}) \odot \mathbf{f}(\mathbf{r} + \mathbf{R})). \quad (119)$$

Both $\mathbf{k}_{1,2}(\mathbf{R})$ can be calculated directly as before; to simplify $\mathbf{k}_3(\mathbf{R})$, we parameterize \mathbf{r} as

$$\mathbf{r} = r \begin{pmatrix} \cos(\theta + \theta_{\mathbf{R}}) \\ \sin(\theta + \theta_{\mathbf{R}}) \end{pmatrix}, \quad (120)$$

and use

$$\mathbf{r} + \mathbf{R} = |\mathbf{r} + \mathbf{R}| \begin{pmatrix} \cos(\theta_{\mathbf{r}+\mathbf{R}}) \\ \sin(\theta_{\mathbf{r}+\mathbf{R}}) \end{pmatrix} = r \begin{pmatrix} \cos(\theta + \theta_{\mathbf{R}}) \\ \sin(\theta + \theta_{\mathbf{R}}) \end{pmatrix} + R \begin{pmatrix} \cos(\theta_{\mathbf{R}}) \\ \sin(\theta_{\mathbf{R}}) \end{pmatrix}. \quad (121)$$

Taking the product of the components of the last equation, we find

$$\cos(\theta_{\mathbf{r}+\mathbf{R}}) \sin(\theta_{\mathbf{r}+\mathbf{R}}) = \frac{(r \cos(\theta + \theta_{\mathbf{R}}) + R \cos(\theta_{\mathbf{R}})) (r \sin(\theta + \theta_{\mathbf{R}}) + R \sin(\theta_{\mathbf{R}}))}{r^2 + R^2 + 2rR \cos(\theta)}. \quad (122)$$

Using this relation, also $\mathbf{k}_3(\mathbf{R})$ can be calculated by MATHEMATICA. We omit the cumbersome results for $\mathbf{k}_{1,2,3}$, and also the result for $\mathbf{a}_{+,2,1}^{(2)}(\mathbf{r}_+)$, given by Eq. (95).

It remains to calculate $\mathbf{a}_{-,2,2}^{(2)}(\mathbf{r}_+)$,

$$\mathbf{a}_{-,2,2}^{(2)}(\mathbf{r}_+) = \frac{1}{\pi^2} \int_{\mathbf{r}, \mathbf{r}'} \frac{\mathbf{r}}{r^2} \frac{(\mathbf{r} + \mathbf{R}) \odot [\hat{\mathbf{z}} \times (\mathbf{r} - \mathbf{r}')] \mathbf{r}' \odot (\mathbf{r}' + \mathbf{R})}{|\mathbf{r} + \mathbf{R}|^2 |\mathbf{r} - \mathbf{r}'|^2 r'^2 |\mathbf{r}' + \mathbf{R}|^2}. \quad (123)$$

Using Eqs. (108) and (109), this can be written as

$$\begin{aligned} \mathbf{a}_{-,2,2}^{(2)}(\mathbf{r}_+) &= \frac{1}{\pi^2} \sum_{n=0}^{\infty} (2 - \delta_{n,0}) \int_{\mathbf{r}, \mathbf{r}'} \frac{1}{r^2 + R^2} \frac{1}{r'^2 + R^2} \frac{1}{|r^2 - r'^2|} \left(\frac{r_{<}}{r_{>}} \right)^n \cos(n(\theta - \theta')) \\ &\quad \times \frac{\mathbf{r}}{r^2 r'^2} \frac{(\mathbf{r} + \mathbf{R}) \odot [\hat{\mathbf{z}} \times (\mathbf{r} - \mathbf{r}')] \mathbf{r}' \odot (\mathbf{r}' + \mathbf{R})}{1 + s \cos(\theta)} \frac{1}{1 + s' \cos(\theta')}. \end{aligned} \quad (124)$$

Repeating similar steps as above, we can get MATHEMATICA to calculate the final result, which is surprisingly simple:

$$\mathbf{a}_{-,2,2}^{(2)}(\mathbf{r}_+) = \frac{1}{2R} \begin{pmatrix} \sin(3\theta_{\mathbf{R}}) \\ \cos(3\theta_{\mathbf{R}}) \end{pmatrix}. \quad (125)$$

For the anisotropic second order correction to the electric field we thus obtain

$$\begin{aligned} \mathbf{E}_-^{(2)}(\mathbf{r}_+) &= -\frac{1}{16} \left[\mathbf{f}(\mathbf{R}) (8 \ln(R/a)^2 - 20 \ln(R/a) + 15 - 8 \cos(4\theta_{\mathbf{R}})) - \frac{6}{R^2} \begin{pmatrix} R_x \\ -R_y \end{pmatrix} \cos(2\theta_{\mathbf{R}}) (4 \ln(R/a) - 5) \right] \\ &\sim -\frac{1}{2} \mathbf{f}(\mathbf{R}) \ln(R/a)^2, \end{aligned} \quad (126)$$

where the asymptotic expansion corresponds to $R \rightarrow \infty$. Remarkably, the dominant contribution at large distances has the same form as in the isotropic case (112). In particular, it is central and potential.

3. Second order correction: mixed terms

Setting $\mathbf{r} = \mathbf{r}_+$ in Eq. (65) we obtain

$$\mathbf{a}_{+-}^{(2)}(\mathbf{r}_+) = -\frac{1}{\pi} \int_{\mathbf{r}} \mathbf{f}(\mathbf{r}) (\mathbf{f}(\mathbf{r}) - \mathbf{f}(\mathbf{r} + \mathbf{R}))^T \left[(\hat{\mathbf{z}} \times \mathbf{a}_-^{(1)}(\mathbf{r} + \mathbf{r}_+)) + \sigma_z (\hat{\mathbf{z}} \times \mathbf{a}_+^{(1)}(\mathbf{r} + \mathbf{r}_+)) \right] = \mathbf{h}_1(\mathbf{R}) + \mathbf{h}_2(\mathbf{R}). \quad (127)$$

Here, we defined

$$\mathbf{h}_1(\mathbf{R}) = -\frac{1}{\pi} \int_{\mathbf{r}} \mathbf{f}(\mathbf{r}) \left[(\mathbf{f}(\mathbf{r}) - \mathbf{f}(\mathbf{r} + \mathbf{R})) \cdot (\hat{\mathbf{z}} \times \mathbf{a}_-^{(1)}(\mathbf{r} + \mathbf{r}_+)) \right], \quad (128)$$

$$\mathbf{h}_2(\mathbf{R}) = -\frac{1}{\pi} \int_{\mathbf{r}} \mathbf{f}(\mathbf{r}) \left[(\mathbf{f}(\mathbf{r}) - \mathbf{f}(\mathbf{r} + \mathbf{R})) \odot (\hat{\mathbf{z}} \times \mathbf{a}_+^{(1)}(\mathbf{r} + \mathbf{r}_+)) \right]. \quad (129)$$

Some further definitions: For $i = 1, 2$ we set

$$\mathbf{h}_i(\mathbf{R}) = \mathbf{h}_{i,1} + \mathbf{h}_{i,2}, \quad (130)$$

where

$$\mathbf{h}_{1,1}(\mathbf{R}) = -\frac{1}{\pi} \int_{\mathbf{r}} \mathbf{f}(\mathbf{r}) \left\{ (\mathbf{f}(\mathbf{r}) - \mathbf{f}(\mathbf{r} + \mathbf{R})) \cdot \left[\hat{\mathbf{z}} \times \left(\mathbf{a}_{-,+}^{(1)}(\mathbf{r} + \mathbf{r}_+) + \mathbf{a}_{-,-}^{(1)}(\mathbf{r} + \mathbf{r}_+) \right) \right] \right\}, \quad (131)$$

$$\mathbf{h}_{1,2}(\mathbf{R}) = \frac{2}{\pi} \int_{\mathbf{r}} \mathbf{f}(\mathbf{r}) \left[(\mathbf{f}(\mathbf{r}) - \mathbf{f}(\mathbf{r} + \mathbf{R})) \cdot \left(\hat{\mathbf{z}} \times \mathbf{a}_{-,+-}^{(1)}(\mathbf{r} + \mathbf{r}_+) \right) \right], \quad (132)$$

$$\mathbf{h}_{2,1}(\mathbf{R}) = -\frac{1}{\pi} \int_{\mathbf{r}} \mathbf{f}(\mathbf{r}) \left\{ (\mathbf{f}(\mathbf{r}) - \mathbf{f}(\mathbf{r} + \mathbf{R})) \odot \left[\hat{\mathbf{z}} \times \left(\mathbf{a}_{+,+}^{(1)}(\mathbf{r} + \mathbf{r}_+) + \mathbf{a}_{+,-}^{(1)}(\mathbf{r} + \mathbf{r}_+) \right) \right] \right\}, \quad (133)$$

$$\mathbf{h}_{2,2}(\mathbf{R}) = \frac{2}{\pi} \int_{\mathbf{r}} \mathbf{f}(\mathbf{r}) \left[(\mathbf{f}(\mathbf{r}) - \mathbf{f}(\mathbf{r} + \mathbf{R})) \odot \left(\hat{\mathbf{z}} \times \mathbf{a}_{+,+-}^{(1)}(\mathbf{r} + \mathbf{r}_+) \right) \right]. \quad (134)$$

In $\mathbf{h}_{1,1}(\mathbf{R})$, we can use Eq. (113), which yields

$$\begin{aligned} \mathbf{h}_{1,1}(\mathbf{R}) &= \frac{1}{\pi} \int_{\mathbf{r}} \mathbf{f}(\mathbf{r}) [(\mathbf{f}(\mathbf{r}) - \mathbf{f}(\mathbf{r} + \mathbf{R})) \cdot (\cos(\theta) \sin(\theta) \mathbf{f}(\mathbf{r}) + \cos(\theta_{\mathbf{r}+\mathbf{R}}) \sin(\theta_{\mathbf{r}+\mathbf{R}}) \mathbf{f}(\mathbf{r} + \mathbf{R}))] \\ &= \mathbf{l}_1(\mathbf{R}) + \mathbf{l}_2(\mathbf{R}) + \mathbf{l}_3(\mathbf{R}), \end{aligned} \quad (135)$$

where

$$\mathbf{l}_1(\mathbf{R}) = \frac{1}{\pi} \int_{\mathbf{r}} \cos(\theta) \sin(\theta) \mathbf{f}(\mathbf{r}) [(\mathbf{f}(\mathbf{r}) - \mathbf{f}(\mathbf{r} + \mathbf{R})) \cdot \mathbf{f}(\mathbf{r})], \quad (136)$$

$$\mathbf{l}_2(\mathbf{R}) = -\frac{1}{\pi} \int_{\mathbf{r}} \cos(\theta_{\mathbf{r}+\mathbf{R}}) \sin(\theta_{\mathbf{r}+\mathbf{R}}) \mathbf{f}(\mathbf{r}) (\mathbf{f}(\mathbf{r} + \mathbf{R}))^2 \quad (137)$$

$$= -\frac{1}{\pi} \int_{\mathbf{r}} \cos(\theta) \sin(\theta) \mathbf{f}(\mathbf{r} - \mathbf{R}) (\mathbf{f}(\mathbf{r}))^2, \quad (138)$$

$$\mathbf{l}_3(\mathbf{R}) = \frac{1}{\pi} \int_{\mathbf{r}} \cos(\theta_{\mathbf{r}+\mathbf{R}}) \sin(\theta_{\mathbf{r}+\mathbf{R}}) \mathbf{f}(\mathbf{r}) (\mathbf{f}(\mathbf{r}) \cdot \mathbf{f}(\mathbf{r} + \mathbf{R})). \quad (139)$$

These quantities are the same as $\mathbf{k}_{1,2,3}$ defined in the previous section up to the replacement of the \odot product with the usual scalar product. The computation of the integrals goes along the same lines as above.

Next, we consider $\mathbf{h}_{1,2}(\mathbf{R})$, which we split into two components,

$$\mathbf{h}_{1,2}(\mathbf{R}) = \mathbf{h}_{1,2,1}(\mathbf{R}) + \mathbf{h}_{1,2,2}(\mathbf{R}), \quad (141)$$

where

$$\mathbf{h}_{1,2,1}(\mathbf{R}) = \frac{2}{\pi} \int_{\mathbf{r}} \mathbf{f}(\mathbf{r}) \left[\mathbf{f}(\mathbf{r}) \cdot \left(\hat{\mathbf{z}} \times \mathbf{a}_{-,+-}^{(1)}(\mathbf{r} + \mathbf{r}_+) \right) \right], \quad (142)$$

$$\mathbf{h}_{1,2,2}(\mathbf{R}) = -\frac{2}{\pi} \int_{\mathbf{r}} \mathbf{f}(\mathbf{r}) \left[\mathbf{f}(\mathbf{r} + \mathbf{R}) \cdot \left(\hat{\mathbf{z}} \times \mathbf{a}_{-,+-}^{(1)}(\mathbf{r} + \mathbf{r}_+) \right) \right]. \quad (143)$$

In the first contribution, we use Eq. (94) and find

$$\mathbf{h}_{1,2,1}(\mathbf{R}) = \frac{1}{\pi^2} \int_{\mathbf{r}, \mathbf{r}'} \mathbf{f}(\mathbf{r}) [\mathbf{f}(\mathbf{r}) \cdot (\hat{\mathbf{z}} \times \mathbf{f}(\mathbf{r} - \mathbf{r}'))] (\mathbf{f}(\mathbf{r}') \odot \mathbf{f}(\mathbf{r}' + \mathbf{R})) = \frac{2}{\pi} \int_{\mathbf{r}'} \mathbf{c}_+(\mathbf{r}') (\mathbf{f}(\mathbf{r}') \odot \mathbf{f}(\mathbf{r}' + \mathbf{R})), \quad (144)$$

where $\mathbf{c}_+(\mathbf{r}')$ is defined in Eq. (96).

We move on to $\mathbf{h}_{1,2,2}(\mathbf{R})$, given by

$$\mathbf{h}_{1,2,2}(\mathbf{R}) = -\frac{1}{\pi^2} \int_{\mathbf{r}, \mathbf{r}'} \mathbf{f}(\mathbf{r}) [\mathbf{f}(\mathbf{r} + \mathbf{R}) \cdot (\hat{\mathbf{z}} \times \mathbf{f}(\mathbf{r} - \mathbf{r}'))] (\mathbf{f}(\mathbf{r}') \odot \mathbf{f}(\mathbf{r}' + \mathbf{R})). \quad (145)$$

Comparison with Eq. (97) shows that $\mathbf{h}_{1,2,2}(\mathbf{R})$ is given by Eq. (124) with the first of the \odot products replaced by the usual scalar product, which yields

$$\mathbf{h}_{1,2,2}(\mathbf{R}) = \frac{1}{2R} \begin{pmatrix} -\sin(3\theta_{\mathbf{R}}) \\ \cos(3\theta_{\mathbf{R}}) \end{pmatrix}. \quad (146)$$

The next on the list is $\mathbf{h}_{2,1}(\mathbf{R})$, which we write — using Eq. (98) — as

$$\mathbf{h}_{2,1}(\mathbf{R}) = -\frac{1}{\pi} \int_{\mathbf{r}} \mathbf{f}(\mathbf{r}) \{(\mathbf{f}(\mathbf{r}) - \mathbf{f}(\mathbf{r} + \mathbf{R})) \odot [\hat{\mathbf{z}} \times (\mathbf{f}(\mathbf{r}) \ln(r/a) + \mathbf{f}(\mathbf{r} + \mathbf{R}) \ln(|\mathbf{r} + \mathbf{R}|/a))]\}. \quad (147)$$

Unfortunately, this can not be simplified as we did above in Eq. (99) because in general $\mathbf{a} \odot (\hat{\mathbf{z}} \times \mathbf{a}) \neq 0$. Hence, we have to invent something new:

$$\mathbf{h}_{2,1}(\mathbf{R}) = \mathbf{m}_1(\mathbf{R}) + \mathbf{m}_2(\mathbf{R}) + \mathbf{m}_3(\mathbf{R}) + \mathbf{m}_4(\mathbf{R}), \quad (148)$$

where

$$\mathbf{m}_1(\mathbf{R}) = -\frac{1}{\pi} \int_{\mathbf{r}} \mathbf{f}(\mathbf{r}) [\mathbf{f}(\mathbf{r}) \odot (\hat{\mathbf{z}} \times \mathbf{f}(\mathbf{r}))] \ln(r/a), \quad (149)$$

$$\mathbf{m}_2(\mathbf{R}) = -\frac{1}{\pi} \int_{\mathbf{r}} \mathbf{f}(\mathbf{r}) [(\mathbf{f}(\mathbf{r}) - \mathbf{f}(\mathbf{r} + \mathbf{R})) \odot (\hat{\mathbf{z}} \times \mathbf{f}(\mathbf{r} + \mathbf{R}))] \ln(|\mathbf{r} + \mathbf{R}|/R) \quad (150)$$

$$= -\frac{1}{\pi} \int_{\mathbf{r}} \mathbf{f}(\mathbf{r} - \mathbf{R}) [(\mathbf{f}(\mathbf{r} - \mathbf{R}) - \mathbf{f}(\mathbf{r})) \odot (\hat{\mathbf{z}} \times \mathbf{f}(\mathbf{r}))] \ln(r/R), \quad (151)$$

$$\mathbf{m}_3(\mathbf{R}) = -\frac{1}{\pi} \ln(R/a) \int_{\mathbf{r}} \mathbf{f}(\mathbf{r}) [(\mathbf{f}(\mathbf{r}) - \mathbf{f}(\mathbf{r} + \mathbf{R})) \odot (\hat{\mathbf{z}} \times \mathbf{f}(\mathbf{r} + \mathbf{R}))], \quad (152)$$

$$\mathbf{m}_4(\mathbf{R}) = \frac{1}{\pi} \int_{\mathbf{r}} \mathbf{f}(\mathbf{r}) [\mathbf{f}(\mathbf{r} + \mathbf{R}) \odot (\hat{\mathbf{z}} \times \mathbf{f}(\mathbf{r}))] \ln(r/a). \quad (153)$$

$\mathbf{m}_1(\mathbf{R})$ vanishes because the integrand is antisymmetric under reflections $\mathbf{r} \rightarrow -\mathbf{r}$.

Now comes $\mathbf{h}_{2,2}(\mathbf{R})$, which again consists of two contributions,

$$\mathbf{h}_{2,2}(\mathbf{R}) = \mathbf{h}_{2,2,1}(\mathbf{R}) + \mathbf{h}_{2,2,2}(\mathbf{R}), \quad (154)$$

where

$$\mathbf{h}_{2,2,1}(\mathbf{R}) = \frac{2}{\pi} \int_{\mathbf{r}} \mathbf{f}(\mathbf{r}) \left[\mathbf{f}(\mathbf{r}) \odot \left(\hat{\mathbf{z}} \times \mathbf{a}_{+,+-}^{(1)}(\mathbf{r} + \mathbf{r}_+) \right) \right], \quad (155)$$

$$\mathbf{h}_{2,2,2}(\mathbf{R}) = -\frac{2}{\pi} \int_{\mathbf{r}} \mathbf{f}(\mathbf{r}) \left[\mathbf{f}(\mathbf{r} + \mathbf{R}) \odot \left(\hat{\mathbf{z}} \times \mathbf{a}_{+,+-}^{(1)}(\mathbf{r} + \mathbf{r}_+) \right) \right]. \quad (156)$$

In the first contribution, we use Eq. (94) and find

$$\begin{aligned} \mathbf{h}_{2,2,1}(\mathbf{R}) &= \frac{1}{\pi^2} \int_{\mathbf{r}, \mathbf{r}'} \mathbf{f}(\mathbf{r}) [\mathbf{f}(\mathbf{r}) \odot (\hat{\mathbf{z}} \times \mathbf{f}(\mathbf{r} - \mathbf{r}'))] (\mathbf{f}(\mathbf{r}') \cdot \mathbf{f}(\mathbf{r}' + \mathbf{R})) \\ &= \frac{2}{\pi} \int_{\mathbf{r}'} \mathbf{c}_-(\mathbf{r}') (\mathbf{f}(\mathbf{r}') \cdot \mathbf{f}(\mathbf{r}' + \mathbf{R})), \end{aligned} \quad (157)$$

where $\mathbf{c}_-(\mathbf{r}')$ is defined in Eq. (96).

Finally, we consider

$$\mathbf{h}_{2,2,2}(\mathbf{R}) = -\frac{1}{\pi^2} \int_{\mathbf{r}, \mathbf{r}'} \mathbf{f}(\mathbf{r}) [\mathbf{f}(\mathbf{r} + \mathbf{R}) \odot (\hat{\mathbf{z}} \times \mathbf{f}(\mathbf{r} - \mathbf{r}'))] (\mathbf{f}(\mathbf{r}') \cdot \mathbf{f}(\mathbf{r}' + \mathbf{R})). \quad (158)$$

Comparing this with Eq. (97) shows that $\mathbf{h}_{2,2,2}(\mathbf{R})$ is given by Eq. (124) with the second of the \odot products replaced by the usual scalar product. We find

$$\mathbf{h}_{2,2,2}(\mathbf{R}) = 0. \quad (159)$$

Combining all of the above results (many of which we haven't stated for brevity), the mixed second order correction to the electric field is thus given by

$$\mathbf{E}_{+-}^{(2)}(\mathbf{r}_+) = \frac{1}{16} \left[2\mathbf{f}(\mathbf{R}) \cos(2\theta_{\mathbf{R}}) (28 \ln(R/a) + 3) + \frac{1}{R^2} \begin{pmatrix} R_x \\ -R_y \end{pmatrix} (8 \ln(R/a)^2 + 12 \ln(R/a) - 5) \right]. \quad (160)$$

4. Numerical checks

some sample parameter values are shown in Figs. 3, 4,

To check the above calculations, we evaluated Eqs. (63), (64), and (65) numerically. The results for

and 5. We find agreement between analytics and numerics up to convergence problems of the numerical integration for select values of \mathbf{r}_+ (the position of the positive charge). The slight discrepancy between results for $\mathbf{E}_{+-}^{(2)}(\mathbf{r}_+)$ and, consequently, $\mathbf{E}^{(2)}(\mathbf{r}_+)$ shown in Figs. 4 and 5, respectively, can be traced back to particularly slow convergence of the numerical integration for integrals of the type of Eq. (152).

III. DYNAMICS OF VORTICES IN THE COMPACT ANISOTROPIC KPZ EQUATION

Having found the electric field acting upon the charges (i.e., vortices) constituting a dipole, we proceed to study the motion of the charges under the influence of Markovian noise. In particular, we are interested in the stationary distribution, which forms the basis of the RG treatment below. The noise acting on the charges originates from the one in the original caKPZ equation, i.e., Eq. (1) in the main text. Hence, the strengths of the noise sources in the caKPZ equation and the equation of motion of vortices are related, but will be renormalized differently [? ?].

A. Equations of motion

As above, we consider a dipole consisting of a positive charge (vortex) at \mathbf{r}_+ , and a negative charge (antivortex) at \mathbf{r}_- . The equations of motion for the vortices read

$$\frac{d\mathbf{r}_\sigma}{dt} = \sigma\mu\mathbf{E}(\mathbf{r}_\sigma) + \boldsymbol{\xi}_\sigma, \quad (161)$$

The first order correction to the electric field is given by (cf. Eqs. (67) and (63); recall that the \odot product becomes the usual scalar product for $\sigma = +$)

$$\mathbf{E}_\sigma^{(1)}(\mathbf{r}_-) = \frac{1}{2\pi} \int_{\mathbf{r}'} \hat{\mathbf{z}} \times \mathbf{f}(\mathbf{r}_- - \mathbf{r}') (\mathbf{f}(\mathbf{r}' - \mathbf{r}_+) - \mathbf{f}(\mathbf{r}' - \mathbf{r}_-)) \odot^2. \quad (166)$$

With a change of the integration variable according to $\mathbf{r}' \rightarrow -\mathbf{r}' + \mathbf{r}_+ + \mathbf{r}_-$, this can be written as

$$\mathbf{E}_\sigma^{(1)}(\mathbf{r}_-) = -\frac{1}{2\pi} \int_{\mathbf{r}'} \hat{\mathbf{z}} \times \mathbf{f}(\mathbf{r}_+ - \mathbf{r}') (\mathbf{f}(\mathbf{r}' - \mathbf{r}_+) - \mathbf{f}(\mathbf{r}' - \mathbf{r}_-)) \odot^2 = -\mathbf{E}_\sigma^{(1)}(\mathbf{r}_+). \quad (167)$$

As stated above, we see the first order correction contributes to Eq. (163) but not to (162).

Finally, let us consider the second order contributions, and here first the diagonal parts. According to Eqs. (67) and (64) it is given by

$$\begin{aligned} \mathbf{E}_\sigma^{(2)}(\mathbf{r}_-) &= \frac{1}{\pi} \int_{\mathbf{r}'} \hat{\mathbf{z}} \times \mathbf{f}(\mathbf{r}_- - \mathbf{r}') \left[(\mathbf{f}(\mathbf{r}' - \mathbf{r}_+) - \mathbf{f}(\mathbf{r}' - \mathbf{r}_-)) \odot \left(\hat{\mathbf{z}} \times \mathbf{a}_\sigma^{(1)}(\mathbf{r}') \right) \right] \\ &= -\frac{1}{\pi} \int_{\mathbf{r}'} \hat{\mathbf{z}} \times \mathbf{f}(\mathbf{r}_+ - \mathbf{r}') \left[(\mathbf{f}(\mathbf{r}' - \mathbf{r}_+) - \mathbf{f}(\mathbf{r}' - \mathbf{r}_-)) \odot \left(\hat{\mathbf{z}} \times \mathbf{a}_\sigma^{(1)}(-\mathbf{r}' + \mathbf{r}_+ + \mathbf{r}_-) \right) \right], \end{aligned} \quad (168)$$

where in the second equality we performed the same change of the integration variable \mathbf{r}' as above. Then, from Eq. (63),

$$\mathbf{a}_\sigma^{(1)}(-\mathbf{r} + \mathbf{r}_+ + \mathbf{r}_-) = \frac{1}{2\pi} \int_{\mathbf{r}'} \mathbf{f}(-\mathbf{r} + \mathbf{r}_+ + \mathbf{r}_- - \mathbf{r}') (\mathbf{f}(\mathbf{r}' - \mathbf{r}_+) - \mathbf{f}(\mathbf{r}' - \mathbf{r}_-)) \odot^2 = -\mathbf{a}_\sigma^{(1)}(\mathbf{r}), \quad (169)$$

where $\sigma = \pm$, cf. Eq. (6) in the main text. As discussed there, the noise correlations read $\langle \xi_{\sigma,i}(t)\xi_{\sigma',j}(t') \rangle = 2\mu T \delta_{\sigma\sigma'} \delta_{ij} \delta(t-t')$, where $\sigma, \sigma' = \pm$, and μ is the vortex mobility. Thus, the relative and ‘‘center-of-mass’’ coordinates, $\mathbf{r} = \mathbf{r}_+ - \mathbf{r}_-$ and $\mathbf{R} = (\mathbf{r}_+ + \mathbf{r}_-)/2$, respectively, obey the following equations of motion:

$$\frac{d\mathbf{r}}{dt} = \mu(\mathbf{E}(\mathbf{r}_+) + \mathbf{E}(\mathbf{r}_-)) + \boldsymbol{\xi}, \quad (162)$$

$$\frac{d\mathbf{R}}{dt} = \frac{\mu}{2}(\mathbf{E}(\mathbf{r}_+) - \mathbf{E}(\mathbf{r}_-)) + \boldsymbol{\Xi}, \quad (163)$$

where $\boldsymbol{\xi} = \boldsymbol{\xi}_+ - \boldsymbol{\xi}_-$ and $\boldsymbol{\Xi} = (\boldsymbol{\xi}_+ + \boldsymbol{\xi}_-)/2$. (To avoid confusion, we note that in the above calculation of the electric field we denoted the relative coordinate by \mathbf{R} .) The correlations of the noise acting on the relative coordinate read

$$\langle \xi_i(t)\xi_j(t') \rangle = \sum_{\sigma,\sigma'} \sigma\sigma' \langle \xi_{\sigma,i}(t)\xi_{\sigma',j}(t') \rangle = 4\mu T \delta_{ij} \delta(t-t'). \quad (164)$$

As we show in the following, the relative coordinate is only affected by the zeroth and second order contributions to the electric field, whereas the first order corrections induces motion of the center of mass.

To this end, for the bare Coulomb interaction, from Eqs. (67) and (57) we find $\mathbf{E}^{(0)}(\mathbf{r}_+) = \mathbf{f}(\mathbf{r}_+ - \mathbf{r}_-)$ (recall that $\mathbf{f}(0) = 0$ due to the short-distance cutoff) and hence

$$\mathbf{E}^{(0)}(\mathbf{r}_-) = -\mathbf{f}(\mathbf{r}_- - \mathbf{r}_+) = \mathbf{f}(\mathbf{r}_+ - \mathbf{r}_-) = \mathbf{E}^{(0)}(\mathbf{r}_+), \quad (165)$$

where we used that $\mathbf{f}(-\mathbf{r}) = -\mathbf{f}(\mathbf{r})$ as can be seen from Eq. (56). Thus, the Coulomb interaction enters Eq. (162) with a factor of two but drops out of the difference in Eq. (163).

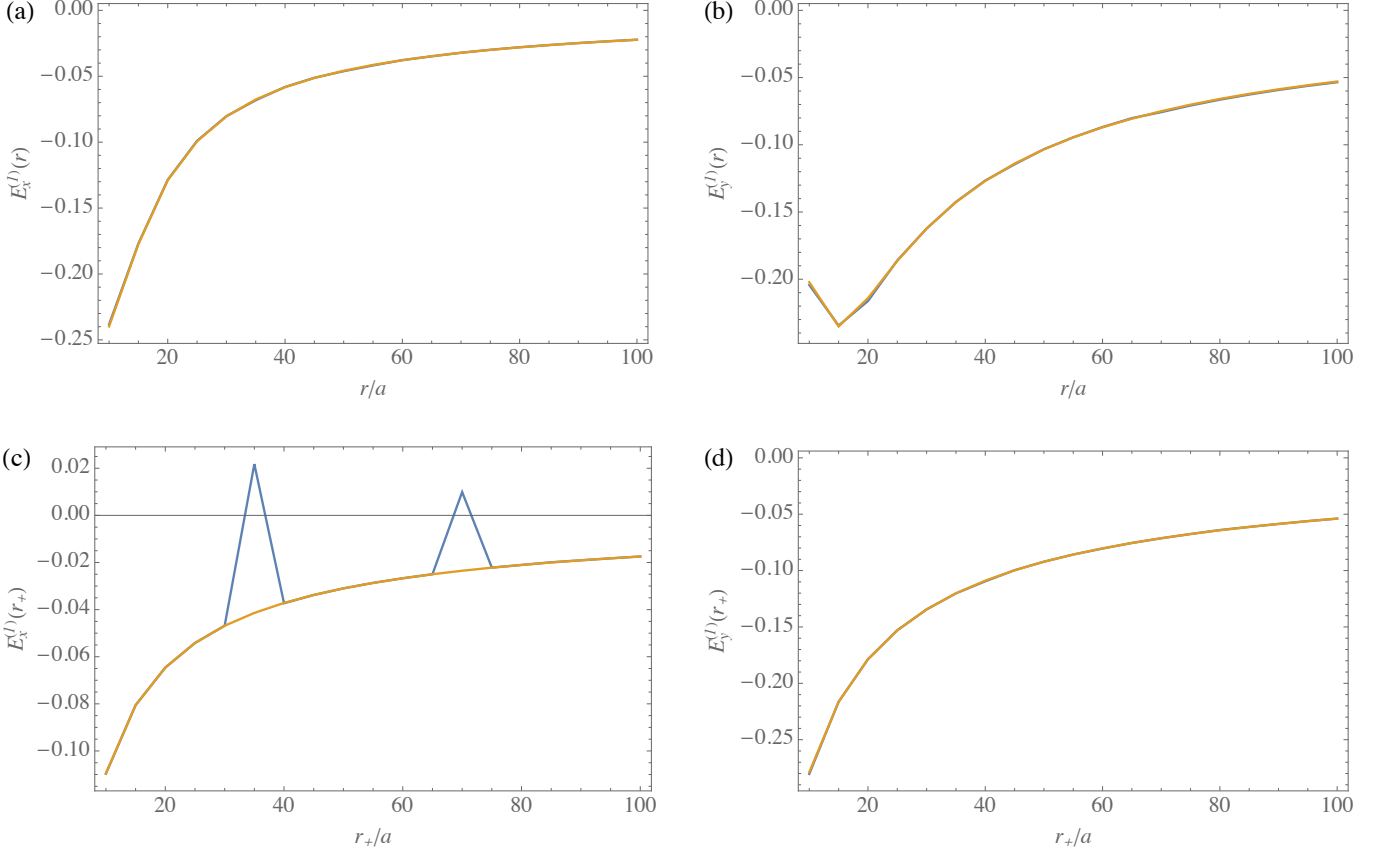


Figure 3. Comparison between analytical (orange lines) and numerical (blue lines) results for the first-order correction to the electric field. (a) and (b) show the x and y components of $\mathbf{E}^{(1)}(\mathbf{r})$ for $\alpha_+ = 1, \alpha_- = 0.7, \mathbf{r} = r(\cos(\theta), \sin(\theta))$ with $\theta = 7\pi/8$, and $\mathbf{r}_+ = r_+(\cos(\theta_+), \sin(\theta_+))$ with $r_+/a = 10, \theta_+ = \pi/5$. In (c) and (d) we plot the components of $\mathbf{E}^{(1)}(\mathbf{r}_+)$ for $\alpha_+ = 1, \alpha_- = -1.2, \theta_+ = 3\pi/4$. For some apparently random values of r_+ in (c) the convergence of the numerical integration is relatively poor. In both plots, the negative charge is located at $\mathbf{r}_- = -\mathbf{r}_+$.

and hence $\mathbf{E}_\sigma^{(2)}(\mathbf{r}_-) = \mathbf{E}_\sigma^{(2)}(\mathbf{r}_+)$. Along the same lines, starting from Eqs. (67) and (65) it is straightforward to see that $\mathbf{E}_{+-}^{(2)}(\mathbf{r}_-) = \mathbf{E}_{+-}^{(2)}(\mathbf{r}_+)$. Thus, we find

$$\frac{d\mathbf{r}}{dt} = 2\mu \left(\frac{1}{\varepsilon} \mathbf{E}^{(0)}(\mathbf{r}_+) + \frac{1}{\varepsilon^3} \mathbf{E}^{(2)}(\mathbf{r}_+) \right) + \boldsymbol{\xi}, \quad (170)$$

$$\frac{d\mathbf{R}}{dt} = \frac{\mu}{\varepsilon^2} \mathbf{E}^{(1)}(\mathbf{r}_+) + \boldsymbol{\Xi}, \quad (171)$$

where

$$\mathbf{E}^{(1)}(\mathbf{r}) = - \sum_{\sigma=\pm} \sigma \alpha_\sigma \mathbf{E}_\sigma^{(1)}, \quad \mathbf{E}^{(2)} = - \sum_{\sigma=\pm} \alpha_\sigma^2 \mathbf{E}_\sigma^{(2)} + \alpha_+ \alpha_- \mathbf{E}_{+-}^{(2)}. \quad (172)$$

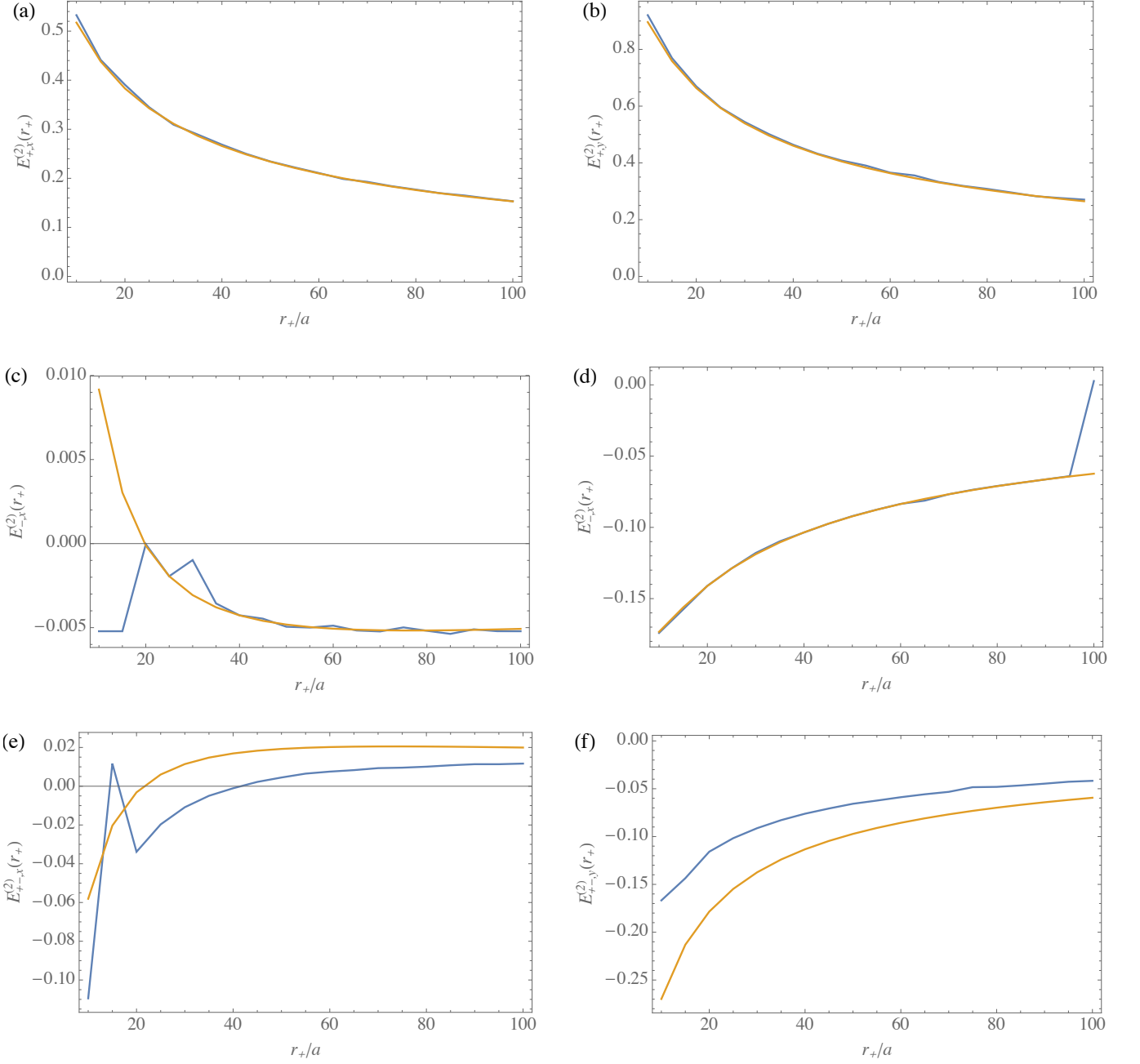


Figure 4. Comparison between analytical (orange lines) and numerical (blue lines) results for the second-order correction to the electric field. (a) and (b) show, respectively, the x and y components of $\mathbf{E}_+^{(2)}(\mathbf{r}_+)$ for $\mathbf{r}_+ = r_+(\cos(\theta_+), \sin(\theta_+))$ with $\theta_+ = \pi/3$. In (c) and (d) are the components of $\mathbf{E}_-^{(2)}(\mathbf{r}_+)$ for $\theta_+ = 2\pi/5$. For some apparently random values of r_+ in (c) and (d) the convergence of the numerical integration is relatively poor. Finally, (e) and (f) are the components of $\mathbf{E}_{+-}^{(2)}(\mathbf{r}_+)$ for $\theta_+ = \pi/8$. In all plots, the negative charge is at $\mathbf{r}_- = -\mathbf{r}_+$.

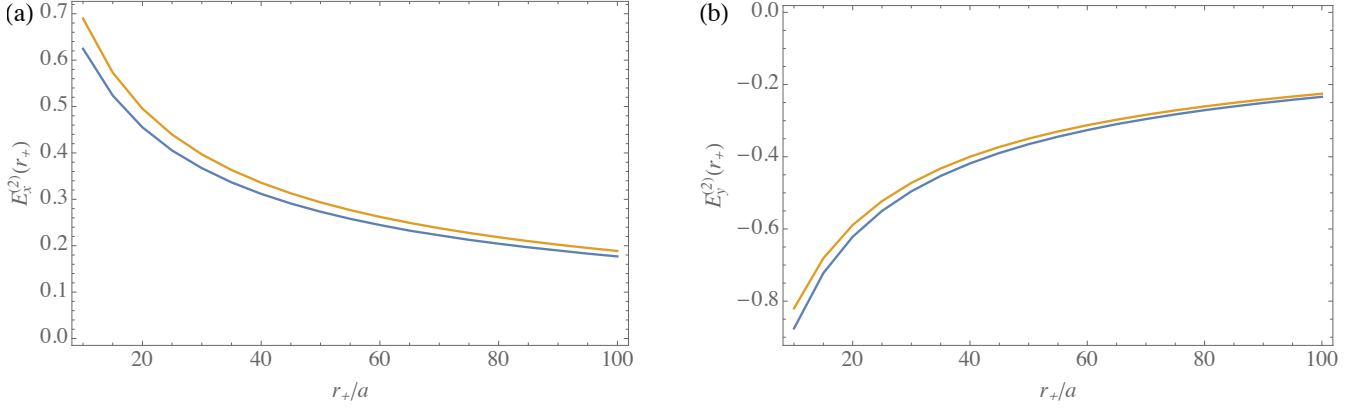


Figure 5. Comparison between analytical (orange lines) and numerical (blue lines) results for the second-order correction to the electric field. (a) and (b) show, respectively, the x and y components of $\mathbf{E}^{(2)}(\mathbf{r}_+)$ for $\alpha_+ = 1, \alpha_- = 0.6, \theta_+ = 5\pi/3$. The negative charge is at $\mathbf{r}_- = -\mathbf{r}_+$.

For convenience, we list again the various contributions to the electric field obtained in the previous section:

$$\begin{aligned}
\mathbf{E}^{(0)}(\mathbf{r}_+) &= \mathbf{f}(\mathbf{r}) = -\frac{\mathbf{r}}{r^2}, \\
\mathbf{E}_+^{(1)}(\mathbf{r}_+) &= \frac{1}{2}\hat{\mathbf{z}} \times \mathbf{f}(\mathbf{r}) (4 \ln(r/a) - 1), \\
\mathbf{E}_-^{(1)}(\mathbf{r}_+) &= \frac{3}{2}\hat{\mathbf{z}} \times \mathbf{f}(\mathbf{r}) \cos(2\theta) - \frac{1}{r^2} \begin{pmatrix} y \\ x \end{pmatrix} (\ln(r/a) - 1), \\
\mathbf{E}_+^{(2)}(\mathbf{r}_+) &= \frac{1}{4}\mathbf{f}(\mathbf{r}) (8 \ln(r/a)^2 + 4 \ln(r/a) - 1), \\
\mathbf{E}_-^{(2)}(\mathbf{r}_+) &= -\frac{1}{16} \left[\mathbf{f}(\mathbf{r}) (8 \ln(r/a)^2 - 20 \ln(r/a) + 15 - 8 \cos(4\theta)) - \frac{6}{r^2} \begin{pmatrix} x \\ -y \end{pmatrix} \cos(2\theta) (4 \ln(r/a) - 5) \right], \\
\mathbf{E}_{+-}^{(2)}(\mathbf{r}_+) &= \frac{1}{16} \left[2\mathbf{f}(\mathbf{r}) \cos(2\theta) (28 \ln(r/a) + 3) + \frac{1}{r^2} \begin{pmatrix} x \\ -y \end{pmatrix} (8 \ln(r/a)^2 + 12 \ln(r/a) - 5) \right],
\end{aligned} \tag{173}$$

where $\mathbf{r} = \mathbf{r}_+ - \mathbf{r}_- = (x, y) = r(\cos(\theta), \sin(\theta))$ is the dipole moment.

Let's consider first the “isotropic” corrections, $\mathbf{E}_+^{(1)}$ and $\mathbf{E}_{++}^{(2)}$, which were previously obtained in Ref. [?]. We note that the first-order correction is perpendicular to the dipole moment and causes motion of the center of mass in this direction, while the second-order term is a central force and adds to the Coulomb force $\mathbf{E}^{(0)}$ affecting the relative motion. Both $\mathbf{E}^{(0)}$ and $\mathbf{E}_{++}^{(2)}$ can be derived from a potential by taking the derivative with respect to the relative coordinate \mathbf{r} . The “anisotropic” and “mixed” second order corrections, $\mathbf{E}_{--}^{(2)}$ and $\mathbf{E}_{+-}^{(2)}$, on the other hand, cannot be derived from a potential. In addition to the central contributions $\propto \mathbf{r}$, they include terms $\propto (x, -y)$ that favor alignment of the dipole along the x or y -axis (depending on the signs of α_+ and α_-). As mentioned in the main text, this is in line with numerical simulations of the anisotropic complex Ginzburg-Landau equation [? ?].

All types of contributions have the common structure of being power series in logarithms. For this reason, perturbation theory is valid up to the scale $L_v \sim ae^{1/\alpha_{\max}}$ where $\alpha_{\max} = \max\{|\alpha_{\pm}|\}$. For distances r which are much larger than the microscopic cutoff but below L_v , $a \ll r \ll L_v$, the second order corrections are dominated by the leading powers of logarithms, $\ln(r/a)^2$. Remarkably, for both $\mathbf{E}_{++}^{(2)}$ and $\mathbf{E}_{--}^{(2)}$ these contributions take the same form, i.e., they are centrally symmetric and potential — in spite of $\mathbf{E}_{--}^{(2)}$ originating from a fully anisotropic non-linearity in the caKPZ equation. The crucial difference between the “isotropic” and “anisotropic” (according to their origin) second order contributions is that the former gives a repulsive correction to the Coulomb force, while the latter gives an *attractive* one.

B. Stationary distribution of a dipole

We proceed to derive the stationary distribution of a dipole subject to the Langevin equation (170). The associated Fokker-Planck equation reads [?]

$$\partial_t \mathcal{P} = -2\mu \nabla \cdot (\mathbf{F} \mathcal{P} - T \nabla \mathcal{P}), \quad (174)$$

with the drift generated by the electric field:

$$\mathbf{F}(\mathbf{r}) = \mathbf{F}^{(0)}(\mathbf{r}) + \mathbf{F}^{(2)}(\mathbf{r}) = \frac{1}{\varepsilon} \mathbf{E}^{(0)}(\mathbf{r}_+) + \frac{1}{\varepsilon^3} \mathbf{E}^{(2)}(\mathbf{r}_+). \quad (175)$$

All the physics below the microscopic cutoff scale a is contained in a single phenomenological parameter, the vortex fugacity y , which quantifies the probability of finding a dipole at the separation a and thus sets the boundary condition for the stationary distribution of the dipole, $\mathcal{P}(\mathbf{r}) = y^2$ for $r = a$. We seek a steady-state solution of Eq. (174) in the form

$$\mathcal{P}(\mathbf{r}) \sim y^2 e^{-\Phi(\mathbf{r})/T}. \quad (176)$$

This is the exact form of the solution in thermal equilibrium, when $\nabla \Phi = \mathbf{F}^{(0)}$ and hence

$$\Phi(\mathbf{r}) = \Phi^{(0)}(\mathbf{r}) = (1/\varepsilon) \ln(r/a). \quad (177)$$

Out of equilibrium, the ansatz (176) yields the leading behavior at low noise strengths [?]. Inserting this ansatz

in the Fokker-Planck equation (174) and expanding the potential as $\Phi = \Phi^{(0)} + \Phi^{(2)}$, where $\Phi^{(0)}$ is the equilibrium solution, results for $T \ll 1$ in

$$\mathbf{F}^{(0)} \cdot (\mathbf{F}^{(2)} + \nabla \Phi^{(2)}) = 0. \quad (178)$$

In order to solve this partial differential equation for $\Phi^{(2)}$ we apply the method of characteristics, which yields the following system of ordinary differential equations:

$$\begin{aligned} \frac{d\mathbf{r}}{dt} &= \mathbf{F}^{(0)}, \\ \frac{d\Phi^{(2)}}{dt} &= -\mathbf{F}^{(0)} \cdot \mathbf{F}^{(2)}. \end{aligned} \quad (179)$$

The integral curves of the first equation flow upstream against the equilibrium part of the drift field, i.e., they are the activation trajectories of the unperturbed equilibrium problem. Integrating the second equation and inserting the first one for $\mathbf{F}^{(0)}$ we get

$$\Phi^{(2)}(\mathbf{r}) = - \int_{t_0}^t dt' \frac{d\mathbf{r}}{dt'} \cdot \mathbf{F}^{(2)} = - \int_{a\hat{\mathbf{r}}}^{\mathbf{r}} ds \cdot \mathbf{F}^{(2)}, \quad (180)$$

where the line integral has to be taken along the activation trajectory of the equilibrium problem that connects $\mathbf{r}(t_0) = a\hat{\mathbf{r}}$ and \mathbf{r} . The initial condition at t_0 is chosen to ensure $\Phi^{(2)}(\mathbf{r}) = 0$ and thus $\mathcal{P}(\mathbf{r}) = y^2$ for $r = a$. We thus find

$$\begin{aligned} \Phi^{(2)}(\mathbf{r}) = -\frac{1}{\varepsilon^3} \left\{ \frac{1}{3} \left(2\alpha_+^2 - \frac{\alpha_-^2}{2} + \frac{\alpha_+ \alpha_-}{2} \cos(2\theta) \right) \ln(r/a)^3 \right. \\ \left. + \frac{1}{2} \left[\alpha_+^2 + \frac{\alpha_-^2}{2} \left(1 - \frac{3}{2} \cos(4\theta) \right) - \frac{11\alpha_+ \alpha_-}{4} \cos(2\theta) \right] \ln(r/a)^2 \right. \\ \left. - \frac{1}{4} \left(\alpha_+^2 - \frac{23\alpha_-^2}{4} \cos(4\theta) + \frac{11\alpha_+ \alpha_-}{4} \cos(2\theta) \right) \ln(r/a) \right\}. \end{aligned} \quad (181)$$

IV. RG FLOW

The ‘‘macroscopic’’ electrodynamics of the previous sections captures the screening of the electric field due to bound vortex-antivortex pairs by introducing the dielectric constant ε . The latter describes the response of the dielectric medium of bound pairs to an electric field. This definition as a response leads to an implicit equation for ε , since the polarization of a single test dipole due to an external electric field is determined by the balance between the external field and the screened Coulomb interaction between the charges constituting the dipole — with the screening in turn determined by ε . The resulting implicit equation for ε can be solved by a renormalization group (RG) approach described in the following.

Section IV A describes the derivation of RG flow equations, which generalizes the one given in Ref. [?] for the isotropic case. We study the phases and fixed points of the RG flow in Sec. IV B. The rather peculiar divergence of the correlation length at the critical point is discussed in Sec. IV C.

A. Derivation of the RG flow equations

As outlined above, in the following we derive an implicit equation for the dielectric constant ε by calculating the polarization of a single test dipole that is induced in linear order by an external electric field. This implicit equation is the starting point from which we obtain a

system of RG flow equations.

Adding an external electric field \mathbf{E}_{eff} in the equations

of motion (161) modifies the potential as $\Phi(\mathbf{r}) \rightarrow \Phi(\mathbf{r}) - \mathbf{E}_{\text{ext}} \cdot \mathbf{r}$. To first order in the external field, the resulting average polarization of our test dipole is given by

$$\langle \mathbf{P} \rangle = \frac{1}{L^2} \int \frac{d^2 \mathbf{R}}{a^2} \frac{d^2 \mathbf{r}}{a^2} \mathbf{r} \mathcal{P}(\mathbf{r}) \left(1 + \frac{1}{T} \mathbf{E}_{\text{ext}} \cdot \mathbf{r} \right) = \frac{1}{T} \int \frac{d^2 \mathbf{r}}{a^2} \mathcal{P}(\mathbf{r}) \frac{\mathbf{r} \mathbf{r}^T}{a^2} \mathbf{E}_{\text{ext}} = \chi \mathbf{E}_{\text{ext}}, \quad (182)$$

which defines the susceptibility tensor χ . In an isotropic system, when $\mathcal{P}(\mathbf{r})$ does not depend on the direction, the susceptibility $\chi \propto \int d^2 \mathbf{r} \mathcal{P}(\mathbf{r}) \mathbf{r} \mathbf{r}^T$ is proportional to the identity matrix, which can be seen by noting that $\mathcal{P}(\mathbf{r})$ is symmetric under (each of the transformations) $x \rightarrow -x, y \rightarrow -y$, and $x \leftrightarrow y$. As can be seen in Eq. (181), the anisotropy we consider here leaves the reflection symmetries under $x \rightarrow -x$ and $y \rightarrow -y$ intact, but breaks the symmetry under the exchange $x \leftrightarrow y$ (note that $\cos(2\theta) = (x^2 - y^2)/r^2$). Hence, the susceptibility tensor χ is still diagonal,

$$\chi = \begin{pmatrix} \chi_x & 0 \\ 0 & \chi_y \end{pmatrix}, \quad (183)$$

but in general its eigenvalues are distinct, $\chi_x \neq \chi_y$. More specifically, we find

$$\begin{pmatrix} \chi_x \\ \chi_y \end{pmatrix} = \frac{y^2}{T} \int_a^\infty \frac{dr}{a} \frac{r^3}{a^3} e^{-\Phi^{(0)}(r)/T} \int_0^{2\pi} d\theta \begin{pmatrix} \cos(\theta)^2 \\ \sin(\theta)^2 \end{pmatrix} e^{-\Phi^{(2)}(\mathbf{r})/T}. \quad (184)$$

We note that strictly speaking the integral over r should be cut at the scale L_v at which the perturbative expansion of the vortex interaction and hence the potential $\Phi(\mathbf{r})$ breaks down. This is assumed implicitly in the following. To make progress with the expression for χ , we expand the last exponential in Eq. (184). This is justified up to parametrically large distances, for which

$$\frac{\alpha_\sigma \alpha_{\sigma'}}{T} \ln(r/a)^3 \ll 1 \quad \iff \quad r \ll L_T = a e^{[T/(\alpha_\sigma \alpha_{\sigma'})]^{1/3}}. \quad (185)$$

where we use the bare value $\varepsilon = 1$ to estimate L_T . We note that for distances below L_T , the temperature is always ‘‘high’’ with regard to the terms $\propto \alpha_\sigma \alpha_{\sigma'}$, which means that by noise-induced fluctuations the test dipole can explore all possible orientations. Only at much larger distances $r \gg L_T$ the test dipole is essentially restricted to the direction that minimizes $\Phi^{(2)}(\mathbf{r})$ with strongly suppressed fluctuations around this direction. Thus, we find ($i = x, y$)

$$\chi_i = \frac{\pi y^2}{T} \int_a^\infty \frac{dr}{a} \frac{r^3}{a^3} e^{-\Phi^{(0)}(r)/T} \left(1 - \frac{1}{\varepsilon^3 T} \sum_{n=1}^3 \beta_{i,n} \ln(r/a)^n \right), \quad (186)$$

with the coefficients

$$\begin{aligned} \beta_{x,1} &= \frac{1}{32} \alpha_+ (8\alpha_+ + 11\alpha_-), & \beta_{x,2} &= -\frac{1}{16} (8\alpha_+^2 - 11\alpha_+ \alpha_- + 4\alpha_-^2), & \beta_{x,3} &= -\frac{1}{12} (8\alpha_+^2 + \alpha_+ \alpha_- - 2\alpha_-^2), \\ \beta_{y,1} &= \frac{1}{32} \alpha_+ (8\alpha_+ - 11\alpha_-), & \beta_{y,2} &= -\frac{1}{16} (8\alpha_+^2 + 11\alpha_+ \alpha_- + 4\alpha_-^2), & \beta_{y,3} &= -\frac{1}{12} (8\alpha_+^2 - \alpha_+ \alpha_- - 2\alpha_-^2). \end{aligned} \quad (187)$$

Despite the noise-induced angular averaging, the coefficients $\beta_{x,n} \neq \beta_{y,n}$ for $n = 1, 2, 3$ if both $\alpha_+, \alpha_- \neq 0$. In consequence, the eigenvalues of the susceptibility tensor are distinct, $\chi_x \neq \chi_y$, and a single dielectric constant ε — as we have assumed in our derivation — is insufficient to describe the resulting anisotropic screening. Remarkably, this complication does not arise in the fully anisotropic configuration in which $\alpha_+ = 0$ (and, of course, also in an isotropic system with $\alpha_- = 0$ a single dielectric constant suffices). In the following, we focus on this case. Then, we find $\chi_x = \chi_y = \chi$, where

$$\chi = \frac{\pi y^2}{T} \int_a^\infty \frac{dr}{a} \left(\frac{r}{a} \right)^{3 - \frac{1}{\varepsilon T}} \left[1 - \frac{\alpha_-^2}{6\varepsilon^3 T} (\ln(r/a)^3 - c \ln(r/a)^2) \right]. \quad (188)$$

Anticipating renormalization of the coefficient of the last term in brackets, we introduced a coupling c with microscopic value $c = 3/2$. The crucial difference between the above expression and the corresponding result in the isotropic case [?

] is the sign of the leading term $\propto \ln(r/a)^3$. This difference brings about major qualitative changes in the behavior of vortices. According to Eq. (38), the renormalized dielectric constant is then

$$\varepsilon_R = \varepsilon + 2\pi\chi = \varepsilon + \frac{2\pi^2 y^2}{T} \int_a^\infty \frac{dr}{a} \left(\frac{r}{a}\right)^{3-\frac{1}{\varepsilon T}} \left[1 - \frac{\alpha_-^2}{6\varepsilon^3 T} (\ln(r/a)^3 - c \ln(r/a)^2)\right]. \quad (189)$$

In the integral on the RHS of this relation, the dielectric constant should be interpreted as the renormalized, scale-dependent value. Thus, Eq. (189) is an implicit integral equation for ε_R . It can be solved by breaking the integral into small steps and absorbing the contribution of each of them progressively in renormalized coefficients. To derive RG differential equations that describe this procedure in the limit of infinitesimal steps, we separate the integral into two parts,

$$\int_a^\infty = \int_a^{a(1+d\ell)} + \int_{a(1+d\ell)}^\infty. \quad (190)$$

The first part is used to redefine ε on a slightly larger cutoff scale $a(1+d\ell)$,

$$\varepsilon' = \varepsilon + \frac{2\pi^2 y^2}{T} d\ell. \quad (191)$$

In the remaining integral, we rescale r to restore the lower limit of integration to a ,

$$\begin{aligned} \varepsilon_R &= \varepsilon' + \frac{2\pi^2 y^2}{T} \int_{a(1+d\ell)}^\infty \frac{dr}{a} \left(\frac{r}{a}\right)^{3-\frac{1}{\varepsilon' T}} \left[1 - \frac{\alpha_-^2}{6\varepsilon'^3 T} (\ln(r/a)^3 - c \ln(r/a)^2)\right] \\ &= \varepsilon' + \frac{2\pi^2 y^2}{T} \int_a^\infty \frac{dr}{a} \left(\frac{r}{a}\right)^{3-\frac{1}{\varepsilon' T}} (1+d\ell)^{4-\frac{1}{\varepsilon' T}} \left[1 - \frac{\alpha_-^2}{6\varepsilon'^3 T} \left(\ln\left(\frac{r(1+d\ell)}{a}\right)^3 - c \ln\left(\frac{r(1+d\ell)}{a}\right)^2\right)\right]. \end{aligned} \quad (192)$$

Expanding in $d\ell$ we find

$$\begin{aligned} (1+d\ell)^{4-\frac{1}{\varepsilon' T}} &= 1 + \left(4 - \frac{1}{\varepsilon' T}\right) d\ell + O(d\ell^2), \\ (\ln(r/a) + \ln(1+d\ell))^n &= \ln(r/a)^n + n \ln(r/a)^{n-1} d\ell + O(d\ell^2). \end{aligned} \quad (193)$$

A redefinition of the other coupling constants is required to bring the expression for ε_R to its original form, Eq. (189),

$$\begin{aligned} \varepsilon_R &= \varepsilon' + \frac{2\pi^2 y^2}{T} \left[1 + \left(4 - \frac{1}{\varepsilon' T}\right) d\ell\right] \int_a^\infty \frac{dr}{a} \left(\frac{r}{a}\right)^{3-\frac{1}{\varepsilon' T}} \left(1 - \frac{c\alpha_-^2}{3\varepsilon'^2} d\ell\right) \left\{1 - \frac{\alpha_-^2}{6\varepsilon'^3 T} [\ln(r/a)^3 - (c - 3d\ell) \ln(r/a)^2]\right\} \\ &= \varepsilon' + \frac{2\pi^2 y'^2}{T'} \int_a^\infty \frac{dr}{a} \left(\frac{r}{a}\right)^{3-\frac{1}{\varepsilon' T'}} \left[1 - \frac{\alpha_-^2}{6\varepsilon'^3 T'} (\ln(r/a)^3 - c' \ln(r/a)^2)\right]. \end{aligned} \quad (194)$$

In the last line, we identified the following renormalized coupling constants:

$$\frac{y'^2}{T'} = \frac{y^2}{T} \left[1 + \left(4 - \frac{1}{\varepsilon' T}\right) d\ell\right] \Rightarrow \frac{d}{d\ell} \left(\frac{y^2}{T}\right) = \left(4 - \frac{1}{\varepsilon' T}\right) \frac{y^2}{T}, \quad (195)$$

$$\frac{1}{T'} = \frac{1}{T} \left(1 - \frac{c\alpha_-^2}{3\varepsilon'^2} d\ell\right) \Rightarrow \frac{d}{d\ell} \frac{1}{T} = -\frac{c\alpha_-^2}{3\varepsilon'^2 T}, \quad (196)$$

$$c' = c - 3d\ell \Rightarrow \frac{dc}{d\ell} = -3. \quad (197)$$

We note that at the given order of y^2 and α_-^2 , all couplings on the RHS of Eq. (194) can be replaced by the renormalized values. The last line can be integrated triv-

ially and yields

$$c = \frac{3}{2} (1 - 2\ell), \quad (198)$$

where the bare value at $\ell = 0$ is $c = 3/2$ as indicated

below Eq. (188). The remaining flow equations read

$$\begin{aligned} \frac{d\varepsilon}{d\ell} &= \frac{2\pi^2 y^2}{T}, \\ \frac{dy}{d\ell} &= \frac{1}{2} \left(4 - \frac{1}{\varepsilon T} + \frac{c\alpha_-^2}{3\varepsilon^2} \right) y, \\ \frac{dT}{d\ell} &= \frac{c\alpha_-^2 T}{3\varepsilon^2}. \end{aligned} \quad (199)$$

This is the form reported in the main text. The appearance of the logarithmic scale ℓ in the flow equations upon inserting Eq. (198) reflects that our perturbative treatment of the non-linearity does not yield the true large-distance behavior of the vortex interaction. For this reason, the RG flow has to be cut when the perturbative corrections become large, i.e., at the scale L_v (or, if it is smaller, at L_T given in Eq. (185) where the angular averaging becomes invalid).

B. Phases and fixed point of the RG flow

To get a feeling for the RG flow described by Eqs. (199), we disregard for the moment that they are valid only up to parametrically large distances, and integrate the flow for a sample of microscopic values. As can be seen in Fig. 6 (and also Fig. 2 of the main text), there is a critical temperature T_c separating two phases with distinct flow patterns. In the low-temperature phase, the dielectric constant approaches a constant value, while the temperature and the fugacity flow to zero. This is in stark contrast to the corresponding phase in the equilibrium KT case, where the temperature is conserved in the RG flow. In fully anisotropic non-equilibrium systems, such a scale-invariant temperature is encountered only asymptotically in the high-temperature phase, when $\varepsilon \sim e^{4\ell}$, $y \sim e^{2\ell}$, and $T \rightarrow T_\infty = \text{const.}$ At large scales, the flow equations simplify as

$$\frac{d\varepsilon}{d\ell} \sim \frac{2\pi^2 y^2}{T_\infty}, \quad \frac{dy}{d\ell} \sim 2y, \quad \frac{dT}{d\ell} \rightarrow 0. \quad (200)$$

This is just the usual KT flow with a renormalized temperature.

The existence of two distinct phases in the RG flow suggests there is a fixed point separating these phases and controlling critical behavior at the transition. In stark contrast to the usual case encountered in continuous phase transitions, the flow equations (199) cannot have a true fixed point since c always grows logarithmically with the running cutoff (i.e., linearly in ℓ). However, as we show in the following, there is nevertheless a fixed point of the flow of a reduced set of logarithmically rescaled variables. To this end, it is convenient to regard the couplings ε , y , and T as functions of

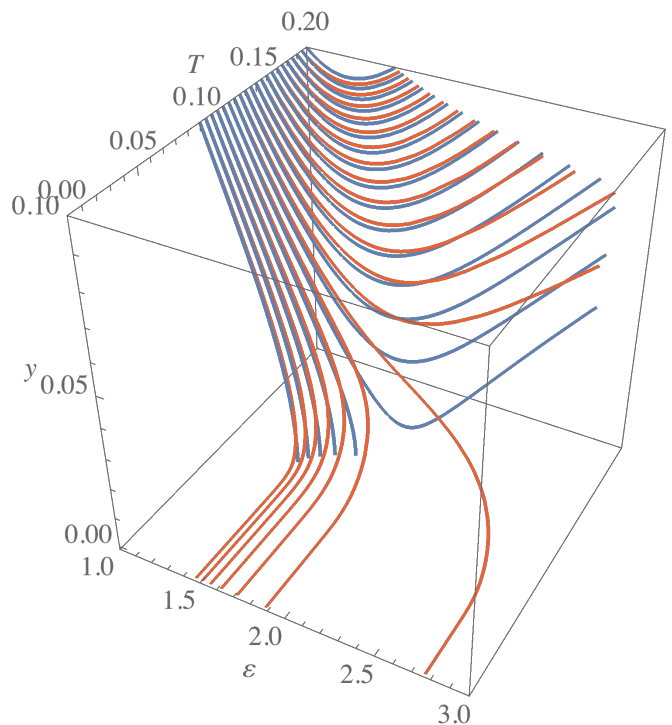


Figure 6. RG flow of ε , y , and T with $\alpha_-^2 = 0.1$ as described by Eqs. (199) (red). Two phases are clearly distinguishable: At low temperatures $T < T_c \approx 0.13$, $y, T \rightarrow 0$ and $\varepsilon \rightarrow \text{const.}$, while at $T > T_c$, $y, \varepsilon \rightarrow \infty$ and $T \rightarrow \text{const.}$ For comparison we show the equilibrium KT flow with $\alpha_-^2 = 0$ (blue). Here, the value of T is conserved in the RG flow. In this figure, the microscopic value of the fugacity is $y = 0.1$, and the temperature is varied from $T = 0.1$ to 0.2 .

$x = -c \in [-3/2, \infty)$ instead of ℓ ,

$$\begin{aligned} \frac{d\varepsilon}{dx} &= \frac{2\pi^2 y^2}{3T}, \\ \frac{dy}{dx} &= \frac{1}{6} \left(4 - \frac{1}{\varepsilon T} - \frac{x\alpha_-^2}{3\varepsilon^2} \right) y, \\ \frac{dT}{dx} &= -\frac{x\alpha_-^2 T}{9\varepsilon^2}. \end{aligned} \quad (201)$$

To find the fixed point of these equations, we effect another change of variables:

$$\tilde{\varepsilon} = \varepsilon/x, \quad \tilde{y} = \sqrt{xy}, \quad \tilde{T} = xT. \quad (202)$$

Strictly speaking, the rescaled variables are ill-defined at the beginning of the flow when $x < 0$. However, here we are concerned with the behavior of the solutions to the flow equations for $x \rightarrow \infty$. The flow equations are then recast as

$$\begin{aligned} \frac{d\tilde{\varepsilon}}{dx} &= \frac{1}{x} \left(\frac{2\pi^2 \tilde{y}^2}{3\tilde{T}} - \tilde{\varepsilon} \right), \\ \frac{d\tilde{y}}{dx} &= \frac{1}{6} \left[4 - \frac{1}{\tilde{\varepsilon}\tilde{T}} + \frac{1}{x} \left(3 - \frac{\alpha_-^2}{3\tilde{\varepsilon}^2} \right) \right] \tilde{y}, \\ \frac{d\tilde{T}}{dx} &= \frac{1}{3x} \left(3 - \frac{\alpha_-^2}{3\tilde{\varepsilon}^2} \right) \tilde{T}. \end{aligned} \quad (203)$$

In this form, it is straightforward to see there is a fixed point at $\tilde{\varepsilon}_*$, \tilde{y}_* , and \tilde{T}_* determined by

$$\frac{2\pi^2\tilde{y}_*^2}{3\tilde{T}_*} - \tilde{\varepsilon}_* = 0, \quad 4 - \frac{1}{\tilde{\varepsilon}_*\tilde{T}_*} = 0, \quad 3 - \frac{\alpha_-^2}{3\tilde{\varepsilon}_*^2} = 0. \quad (204)$$

We find

$$\tilde{\varepsilon}_* = \frac{|\alpha_-|}{3}, \quad \tilde{y}_* = \sqrt{\frac{3}{8}} \frac{1}{\pi}, \quad \tilde{T}_* = \frac{3}{4|\alpha_-|}. \quad (205)$$

Flow trajectories close to criticality are shown in Fig. 7, both for the original and rescaled couplings (202) (see panels (a-c) and (d-f), respectively). The rescaled couplings are close to their fixed-point values in the range $30 \lesssim \ell \lesssim 90$, during which the original ones evolve according to Eq. (202). This logarithmic flow is the origin of the peculiar singularity of the correlation length ξ at the critical point which is distinct from both the algebraic scaling at conventional second order phase transitions, and the essential singularity at the equilibrium KT transition. In the next section, we discuss how the singularity of the correlation length can be inferred from the a linearization of the flow around the fixed point (205).

C. Asymptotic analysis of the linearized flow equations

As usual, we define the correlation length ξ as the scale on which the renormalized fugacity reaches the value $y_1 = 1$. We fix the microscopic value y_0 and regard the temperature T as the tuning parameter through the transition. The origin of the singularity of ξ as $T \rightarrow T_c$ is apparent from panels (b) and (e) in Fig. 7 which show the flow of y and \tilde{y} , respectively. This flow can be divided into three stages: (i) for $0 \leq \ell < \ell_0$ the rescaled fugacity \tilde{y} approaches its fixed-point value \tilde{y}_* and (ii) stays close to this value for $\ell_0 \leq \ell < \ell_1$; eventually, (iii) \tilde{y} flows away from the fixed point and y grows strongly until it reaches $y_1 = 1$ for $\ell_1 \leq \ell \leq \ell_2$. When $T \rightarrow T_c$, $\ell_1 \rightarrow \infty$, while ℓ_0 and $\ell_2 - \ell_1$ remain finite, and therefore $\xi \sim ae^{\ell_2}$. Consequently, to determine the singularity of ξ , it is sufficient to consider stage (ii) of the flow in the vicinity of the fixed point where we can linearize the flow equations.

We collect the deviations from the fixed point in the variable $\mathbf{a} = (\delta\tilde{\varepsilon}, \delta\tilde{y}, \delta\tilde{T}) = (\tilde{\varepsilon} - \tilde{\varepsilon}_*, \tilde{y} - \tilde{y}_*, \tilde{T} - \tilde{T}_*)$. The linearized flow equations read

$$\frac{d\mathbf{a}}{dx} = A\mathbf{a}, \quad A = A_0 + \frac{A_1}{x}, \quad (206)$$

where

$$A_0 = \begin{pmatrix} 0 & 0 & 0 \\ -\sqrt{\frac{3}{2}} \frac{1}{\pi\alpha_-} & 0 & -\sqrt{\frac{2}{3}} \frac{2\alpha_-}{3\pi} \\ 0 & 0 & 0 \end{pmatrix}, \quad (207)$$

$$A_1 = \begin{pmatrix} -1 & \sqrt{\frac{2}{3}} \frac{4\pi\alpha_-}{3} & -\frac{4\alpha_-^2}{9} \\ \sqrt{\frac{3}{2}} \frac{3}{2\pi\alpha_-} & 0 & 0 \\ \frac{9}{2\alpha_-^2} & 0 & 0 \end{pmatrix}.$$

Note that these equations still depend on x and thus cannot be solved straightforwardly. However, since $\ell_2 \gg 1$ when $t = (T - T_c)/T_c \ll 1$, we only need to know the asymptotic behavior of the solution for $x \sim 3\ell \rightarrow \infty$. To solve this problem, we closely follow the method described in Ref. [?].

What makes finding an asymptotic expansion of the solution to Eq. (206) slightly complicated is first that $x = \infty$ is an irregular singular point of this equation and second that A_0 , the leading matrix for $x \rightarrow \infty$, has only one eigenvalue. In the following, we apply a series of transformations to bring Eq. (206) to a form in which the leading matrix has three distinct eigenvalues. Then, the leading matrix can be diagonalized, which results in three decoupled equations that can be integrated straightforwardly.

The first step is to bring A_0 to Jordan normal form by means of a transformation P_1 ,

$$\mathbf{a}_1 = P_1^{-1}\mathbf{a}, \quad \frac{d\mathbf{a}_1}{dx} = A_1\mathbf{a}_1, \quad A_1 = P_1^{-1}AP_1 = A_{10} + \frac{A_{11}}{x}, \quad (208)$$

where

$$P_1 = \begin{pmatrix} -\frac{4\alpha_-^2}{9} & 0 & \sqrt{\frac{2}{3}}\pi\alpha_- \\ 0 & 1 & 0 \\ 1 & 0 & 0 \end{pmatrix}, \quad A_{10} = \begin{pmatrix} 0 & 0 & 0 \\ 0 & 0 & 1 \\ 0 & 0 & 0 \end{pmatrix}, \quad (209)$$

$$A_{11} = \begin{pmatrix} -2 & 0 & \sqrt{\frac{3}{2}} \frac{3\pi}{\alpha_-} \\ \sqrt{\frac{2}{3}} \frac{\alpha_-}{\pi} & 0 & \frac{3}{2} \\ -\sqrt{\frac{2}{3}} \frac{4\alpha_-}{3\pi} & \frac{4}{3} & 1 \end{pmatrix}. \quad (210)$$

The matrix $A_{10} = H_1 \oplus H_2$ is the direct sum of two shifting matrices, which are matrices with ones on the superdiagonal and zeroes elsewhere, $H_1 = 0$ and $H_2 = \begin{pmatrix} 0 & 1 \\ 0 & 0 \end{pmatrix}$. We next apply a transformation P_2 to bring the sub-leading matrix A_{11} to a form in which the only non-zero entries occur in the rows corresponding to the last rows of the blocks $H_{1,2}$, i.e.,

$$\mathbf{a}_2 = P_2^{-1}\mathbf{a}_1, \quad \frac{d\mathbf{a}_2}{dx} = A_2\mathbf{a}_2, \quad A_2 = P_2^{-1}A_1P_2 - P_2^{-1} \frac{dP_2}{dx}, \quad (211)$$

where the matrix A_2 has the structure

$$A_2 = \begin{pmatrix} A_{211} & A_{212} & A_{213} \\ 0 & 0 & 1 \\ A_{231} & A_{232} & A_{233} \end{pmatrix}. \quad (212)$$

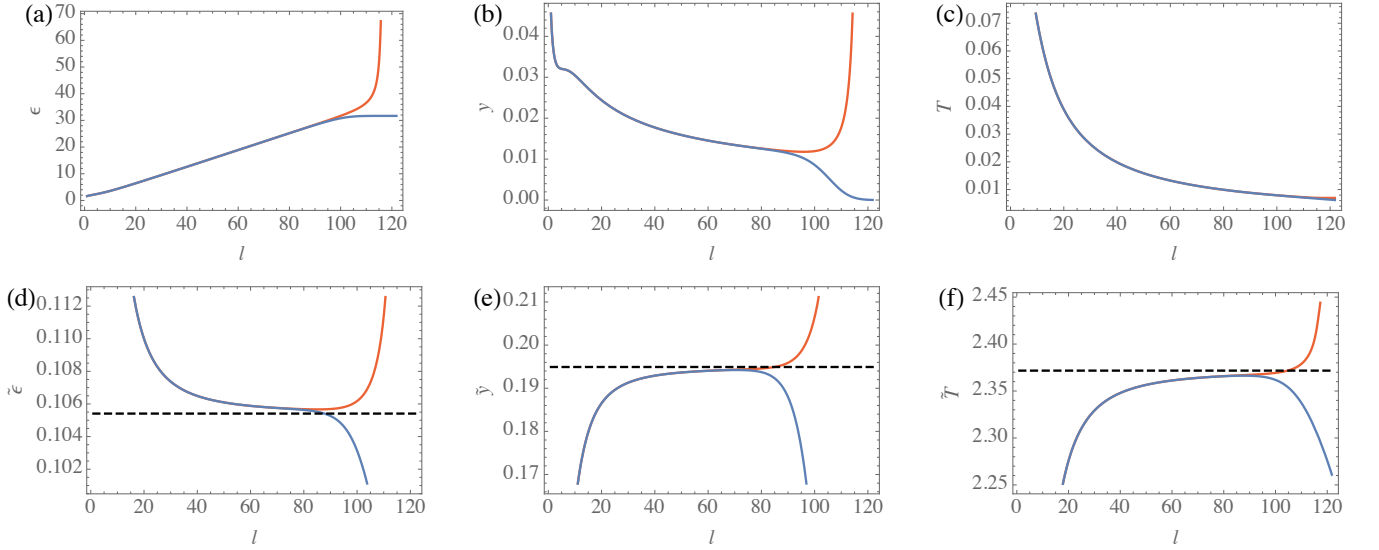


Figure 7. RG flow slightly above and below the critical temperature (red and blue solid lines, respectively). Panels (a-c) show the RG flow in terms of ε , y , and T , while in panels (d-f) the rescaled couplings defined in Eq. (202) are plotted. Black dashed lines indicate the critical values given in Eq. (205).

Inserting in Eq. (211) the asymptotic ansätze $P_2 \sim \sum_{r=0}^{\infty} P_{2r}/x^r$ and $A_2 \sim \sum_{r=0}^{\infty} A_{2r}/x^r$ and identifying coefficients of the same powers of x , we obtain $A_{10}P_{20} - P_{20}A_{20} = 0$ and

$$A_{10}P_{2r} - P_{2r}A_{20} = \sum_{s=0}^{r-1} (P_{2s}A_{2,r-s} - A_{1,r-s}P_{2s}) - (r-1)P_{2,r-1}. \quad (213)$$

The first relation can be solved by setting $A_{20} = A_{10}$ and $P_{20} = 1$; the second relation determines A_{2r} and P_{2r} for $r \geq 1$ recursively. We obtain the desired transformation by restricting the form of P_{2r} with $r \geq 1$ as

$$P_{2r} = \begin{pmatrix} 0 & 0 & 0 \\ 0 & P_{222r} & 0 \\ P_{231r} & P_{232r} & 0 \end{pmatrix}. \quad (214)$$

Insertion of Eqs. (212) and (214) in Eq. (213) yields a sequence of linear equations for the elements of A_2 and P_2 that can be solved straightforwardly to any desired order. We omit the explicit expressions. Next, we apply a first shearing transformation,

$$\mathbf{a}_3 = P_3^{-1} \mathbf{a}_2, \quad \frac{d\mathbf{a}_3}{dx} = A_3 \mathbf{a}_3, \quad (215)$$

where

$$A_3 = P_3^{-1} A_2 P_3 - P_3^{-1} \frac{dP_3}{dx}, \quad (216)$$

$$P_3 = \text{diag}(1, x^{-g_1}, x^{-2g_1}).$$

We choose $g_1 = 1/3$ (this choice is, of course, not arbitrary, but is determined by a well-defined procedure [?

]), and to bring the equation back to a form that involves only integer powers of the variables, we switch to $x = \alpha_1 y^{p_1}$, where $\alpha_1 = p_1^{1/(g_1-1)}$ and $p_1 = 3$. This yields

$$\frac{1}{y} \frac{d\mathbf{a}_3}{dy} = \tilde{A}_3 \mathbf{a}_3, \quad \tilde{A}_3 = x^{g_1} A_3. \quad (217)$$

The leading matrix in the last equation, $\tilde{A}_{30} = \lim_{y \rightarrow \infty} \tilde{A}_3$, still has only one distinct eigenvalue, and it seems as if we would not have gained anything. However, we must not despair. Instead, we bring \tilde{A}_{30} again to Jordan normal form,

$$\mathbf{a}_4 = P_4^{-1} \mathbf{a}_3, \quad \frac{1}{y} \frac{d\mathbf{a}_4}{dy} = A_4 \mathbf{a}_4, \quad A_4 = P_4^{-1} \tilde{A}_3 P_4, \quad (218)$$

with

$$P_4 = \begin{pmatrix} 0 & 0 & -\sqrt{\frac{3}{2}} \frac{3\pi}{4\alpha_1} \\ 1 & 0 & 0 \\ 0 & 1 & 0 \end{pmatrix}, \quad (219)$$

and perform a second shearing transformation,

$$\mathbf{a}_5 = P_5^{-1} \mathbf{a}_4, \quad \frac{1}{y} \frac{d\mathbf{a}_5}{dy} = A_5 \mathbf{a}_5, \quad (220)$$

where

$$A_5 = P_5^{-1} A_4 P_5 - \frac{1}{y} P_5^{-1} \frac{dP_5}{dy}, \quad (221)$$

$$P_5 = \text{diag}(1, y^{-g_2}, y^{-2g_2}).$$

This time, we choose $g_2 = 1/2$, and another change of variables $y = \alpha_2 z^{p_2}$ with $\alpha_2 = p_2^{1/(g_2-2)}$ and $p_2 = 2$ brings us to

$$\frac{1}{z^2} \frac{d\mathbf{a}_5}{dz} = \tilde{A}_5 \mathbf{a}_5, \quad \tilde{A}_5 = y^{g_2} A_5. \quad (222)$$

Miraculously, $\tilde{A}_{50} = \lim_{z \rightarrow \infty} \tilde{A}_5$ has three distinct eigenvalues, 0 and $\pm 2/3^{1/4}$. Hence, we can now go ahead and diagonalize \tilde{A}_5 order by order in $1/z$. The first step is to diagonalize the leading matrix \tilde{A}_{50} ,

$$\mathbf{a}_6 = P_6^{-1} \mathbf{a}_5, \quad \frac{1}{z^2} \frac{d\mathbf{a}_6}{dz} = A_6 \mathbf{a}_6, \quad A_6 = P_6^{-1} \tilde{A}_5 P_6, \quad (223)$$

where

$$P_6 = \begin{pmatrix} -\frac{3^{1/4}}{2} & \frac{3^{1/4}}{2} & -\frac{\sqrt{3}}{4} \\ 1 & 1 & 0 \\ 0 & 0 & 1 \end{pmatrix}. \quad (224)$$

We move on to diagonalize the sub-leading parts of A_6 in two steps,

$$\mathbf{a}_7 = P_7^{-1} \mathbf{a}_6, \quad \frac{1}{z^2} \frac{d\mathbf{a}_7}{dz} = A_7 \mathbf{a}_7, \quad (225)$$

$$A_7 = P_7^{-1} A_6 P_7 - \frac{1}{z^2} P_7^{-1} \frac{dP_7}{dz}, \quad (226)$$

and

$$\mathbf{a}_8 = P_8^{-1} \mathbf{a}_7, \quad \frac{1}{z^2} \frac{d\mathbf{a}_8}{dz} = A_8 \mathbf{a}_8, \quad (227)$$

$$A_8 = P_8^{-1} A_7 P_8 - \frac{1}{z^2} P_8^{-1} \frac{dP_8}{dz}. \quad (228)$$

The matrices $A_{7,8}$ and $P_{7,8}$ can be found order by order in $1/z$ by recursion relations similar to Eq. (213). They take the forms

$$A_7 = \begin{pmatrix} A_{711} & 0 & 0 \\ 0 & A_{722} & A_{723} \\ 0 & A_{732} & A_{733} \end{pmatrix}, \quad P_7 = \begin{pmatrix} 0 & P_{712} & P_{713} \\ P_{721} & 0 & 0 \\ P_{731} & 0 & 0 \end{pmatrix}, \quad (229)$$

$$P_8 = \begin{pmatrix} 1 & 0 & 0 \\ 0 & 0 & P_{823} \\ 0 & P_{832} & 0 \end{pmatrix}, \quad (230)$$

and A_8 is diagonal. The general solution to Eq. (227) is thus

$$\mathbf{a}_8(z) = e^{\int_{z_0}^z dz' z'^2 A_8(z')} \mathbf{a}_{80} \sim e^{\int_{z_0}^z dz' z'^2 A_8^\infty(z')} D_8^\infty \mathbf{a}_{80}. \quad (231)$$

In the last equation, in A_8^∞ we keep terms in the asymptotic expansion of A_8 up to order $O(1/z^3)$ so that the lowest order term in the exponent is $O(\ln(z))$ — this is the order to which we have to perform all the above transformations to find the leading asymptotic behavior. D_8^∞ is a constant diagonal matrix which could only be found by carrying out the above analysis *exactly* (not just asymptotically) since every order of $1/z$ in A_8 contributes to D_8^∞ . However, the precise value of D_8^∞ is not important for our purposes. From Eq. (231), we can

reconstruct $\mathbf{a}(x)$ by undoing all transformations:

$$\begin{aligned} \mathbf{a}(x) &= P_1 P_2 P_3 P_4 P_5 P_6 P_7 P_8 \mathbf{a}_8(z) \\ &\sim P_1 P_2 P_3 P_4 P_5 P_6 P_7 P_8 e^{\int_{z_0}^z dz' z'^2 A_8^\infty(z')} D_8^\infty \mathbf{a}_{80}, \end{aligned} \quad (232)$$

where

$$z = \left[\frac{1}{\alpha_2} \left(\frac{x}{\alpha_1} \right)^{1/p_1} \right]^{1/p_2}. \quad (233)$$

We find, for $x \rightarrow \infty$,

$$\begin{aligned} \delta\tilde{\varepsilon} &\sim x^{1/4} e^{4\sqrt{x/3}}, \\ \delta\tilde{y} &\sim x^{3/4} e^{4\sqrt{x/3}}, \\ \delta\tilde{T} &\sim x^{-1/4} e^{4\sqrt{x/3}}. \end{aligned} \quad (234)$$

As we demonstrate in Fig. 8, these asymptotic expressions give an excellent approximation to the exact solution of the linearized flow equation (206) even at relatively small values of x . The corresponding asymptotic behavior of the original couplings follows from Eq. (202) and $x = 3/2(2\ell - 1) \sim 3\ell$,

$$\begin{aligned} \varepsilon &\sim \delta\varepsilon_\infty = \delta\varepsilon_{\infty,0} \ell^{5/4} e^{4\sqrt{\ell}}, \\ y &\sim \delta y_\infty = \delta y_{\infty,0} \ell^{1/4} e^{4\sqrt{\ell}}, \\ T &\sim \delta T_\infty = \delta T_{\infty,0} \ell^{-5/4} e^{4\sqrt{\ell}}. \end{aligned} \quad (235)$$

At $T = T_c$, the couplings flow to the fixed point, and $\delta\varepsilon_{\infty,0} = \delta y_{\infty,0} = \delta T_{\infty,0} = 0$. Close to criticality, when $t = (T - T_c)/T_c \ll 1$, we expect that the amplitudes $\varepsilon_{\infty,0}$, $\delta y_{\infty,0}$, and $\delta T_{\infty,0}$ in Eq. (235) are proportional to t . In particular, setting $\delta y_\infty \propto t$, the correlation length is $\xi = ae^\ell$ where

$$\begin{aligned} 4\sqrt{\ell} + \frac{1}{4} \ln(\ell) &\sim -\ln(t) \\ \Rightarrow \ln(\xi/a) &\sim \frac{1}{16} \ln(t) (\ln(t) + \ln(|\ln(t)|)). \end{aligned} \quad (236)$$

This type of singularity is between true scaling behavior encountered at a second order phase transition and the essential singularity of ξ at the equilibrium KT transition:

$$\begin{aligned} \text{true scaling:} & \quad \frac{1}{\nu} \ell \sim -\ln(t) \Rightarrow \xi/a \sim t^{-\nu}, \\ \text{equilibrium KT:} & \quad 2 \ln(\ell) \sim -\ln(t) \Rightarrow \xi/a \sim e^{C/\sqrt{t}}. \end{aligned} \quad (237)$$

A comparison showing the good agreement between our analytical prediction (236) and the correlation length obtained from a numerical integration of the flow equations is shown in Fig. 9.

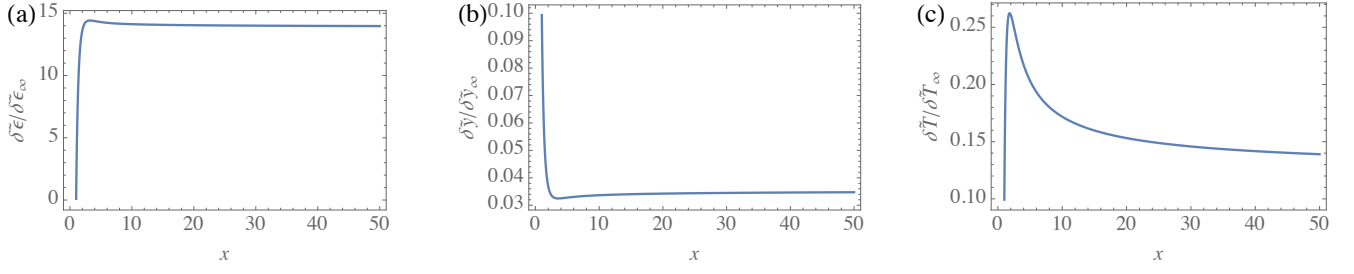


Figure 8. Comparison between the numerical solution of the linearized flow equations (206) and the asymptotic expansion (234). For the numerical integration, we chose initial values $\delta\tilde{\varepsilon} = \delta\tilde{y} = \delta\tilde{T} = 1$. Division by the asymptotic expressions shows that the solution is well described by the asymptotic behavior already for small values of $x \lesssim 10$. Asymptotic analysis does not determine the prefactors in Eq. (234), hence we arbitrarily set them to one. (For the correct value, the plotted curves would approach 1 for $x \rightarrow \infty$.)

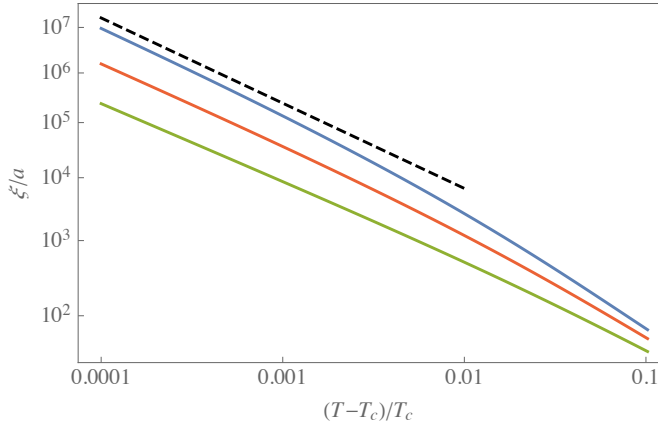


Figure 9. Divergence of the correlation length at the critical temperature for $\alpha_c^2 = 0.1, 0.2, 0.5$ (top to bottom). The vertical axis is rescaled as $4\sqrt{\ln(\xi/a)} + \ln(\ln(\xi/a))/4$ (cf. Eq. (236)) so that the curves approach straight lines with slope -1 as $T \rightarrow T_c$ (for comparison shown as black dashed line).